Int J Earth Sci (Geol Rundsch)
DOI 10.1007/s00531-013-0923-3

ORIGINAL PAPER

The Ediacaran–Early Cambrian detrital zircon record of NW Iberia: possible sources and paleogeographic constraints

J. Fernández-Suárez · G. Gutiérrez-Alonso · D. Pastor-Galán · M. Hofmann · J. B. Murphy · U. Linnemann

Received: 29 January 2013 / Accepted: 29 May 2013

Abstract Ediacaran and Early Cambrian sedimentary rocks from NW Iberia have been investigated for detrital zircon U–Pb ages. A total of 1,161 concordant U–Pb ages were obtained in zircons separated from four Ediacaran samples (3 from the Cantabrian Zone and one from the Central Iberian zone) and two Lower Cambrian samples (one from the Cantabrian Zone and one from the Central Iberian Zone). Major and trace elements including REE and Sm–Nd isotopes were also analyzed on the same set of samples. The stratigraphically older Ediacaran sequence in the Cantabrian Zone has a maximum sedimentation age of ca. 600 Ma based on detrital zircon content and is intruded by ca. 590–580 Ma granitoids constraining the deposition of this part of the sequence between ca. 600 and 580 Ma. The stratigraphically younger Ediacaran sequence in the Cantabrian Zone has a maximum sedimentation age of ca. 553 Ma. The Ediacaran sample from the Central Iberian Zone has an identical within error maximum sedimentation age of ca. 555 Ma. The detrital zircon U–Pb age patterns are very similar in all the Ediacaran samples from both zones including the main age groups ca. 0.55–0.75 Ga, ca. 0.85–1.15 Ga and minor Paleoproterozoic (ca. 1.9–2.1 Ga) and Archean (ca. 2.4–2.6 Ga) populations. Kolmogorov–Smirnov statistical tests performed on this set of samples indicate that they all were derived from the same parent population (i.e., same source area). The same can be said on the basis of Nd isotopes, REE patterns and trace element concentrations. The two Cambrian samples, however, show contrasting signatures: The sample from the Cantabrian Zone lacks the ca. 0.85–1.15 Ga population and has a high proportion of Paleoproterozoic and Archean zircons (>60 %) and a more negative ε_{Nd} and higher T_{DM} values than the Ediacaran samples. The Early Cambrian sample from the Central Iberian Zone has the same U–Pb detrital zircon age distribution (based on KS tests) as all the Ediacaran samples but has a significantly more negative ε_{Nd} value. These data suggest apparently continuous sedimentation in the NW Iberian realm of northern Gondwana between ca. 600 and 550 Ma and changes in the detrital influx around the Ediacaran–Cambrian boundary. The nature and origin of these changes cannot be determined with available data, but they must involve tectonic activity on the margin as evidenced by the angular unconformity separating the Ediacaran and Lower Cambrian strata in the Cantabrian Zone. The absence of this unconformity and the apparent continuity of detrital zircon age distribution between Ediacaran and Cambrian rocks in the Central Iberian Zone suggest that the margin became segmented with significant transport and sedimentation flux changes in relatively short distances. As to the paleoposition of NW Iberia in Ediacaran–Early Cambrian times, comparison of the data presented herein with a wealth of relevant data

Electronic supplementary material The online version of this article (doi:10.1007/s00531-013-0923-3) contains supplementary material, which is available to authorized users.

J. Fernández-Suárez (✉)
Departamento de Petrología y Geoquímica, Universidad Complutense and IGEO-CSIC, 28040 Madrid, Spain
e-mail: jfsuarez@geo.ucm.es

G. Gutiérrez-Alonso · D. Pastor-Galán
Departamento de Geología, Universidad de Salamanca, Plaza de los Caídos s/n, 37008 Salamanca, Spain

M. Hofmann · U. Linnemann
Senckenberg Naturhistorische Sammlungen Dresden, Königsbrücker Landstr. 159, 01109 Dresden, Germany

J. B. Murphy
Department of Earth Sciences, St. Francis Xavier University, Antigonish, NS B2G 2W5, Canada

Published online: 16 June 2013

from the literature both on the European peri-Gondwanan terranes and on the terranes of northern Africa suggests that NW Iberia may have lain closer to the present-day Egypt–Israel–Jordan area and that the potential source of the hitherto enigmatic Tonian–Stenian zircons could be traced to exposed segments of arc terranes such as that described in the Sinai Peninsula (Be'eri-Shlevin et al. in Geology 40:403–406, 2012).

Keywords Iberia · Ediacaran · Cambrian · Paleogeography · Detrital zircon · U–Pb geochronology

Introduction

The origin, paleoposition and nature of the pre-Ediacaran basement of Iberia have been a subject of particular interest since the first findings of late Mesoproterozoic–Early Neoproterozoic (Stenian–Tonian) detrital zircons in the Ediacaran and Lower Paleozoic sedimentary rocks cropping out in NW Iberia (Fernández-Suárez et al. 1999, 2000; Gutiérrez-Alonso et al. 2003). In the aforementioned studies, NW Iberia was interpreted to have lain adjacent to the Amazonian Craton in Ediacaran–Early Paleozoic times. This hypothesis relied heavily on the observation that there were no other known sources for ca. 1.0 Ga zircons in the northern margin of Gondwana. The involvement of a Tonian–Stenian source in the genesis of the Ediacaran and Paleozoic clastic rocks of NW Iberia was found to be in contrast with the sources involved in the genesis of coeval clastic rocks in SW Iberia and Brittany (Fernández-Suárez et al. 2002a, b; Samson et al. 2005) where the Tonian–Stenian zircons were either absent or mere "accidental" occurrences (<0.5 % of the population). These observations argued for a ca 1.0 Ga basement terrane to have docked to the NW margin of Gondwana, near the West African Craton, at Ediacaran–Cambrian boundary times. Subsequently, further work on detrital zircons and micas on rocks of Paleozoic age (Fernández-Suárez et al. 2002a, b; Martínez Catalán et al. 2004; Gutiérrez-Alonso et al. 2005; Shaw et al. 2012a; Pastor-Galán et al. 2012b; Ábalos et al. 2012; Pereira et al. 2012a, b) confirmed the abundance of such Tonian–Stenian sources and an increase in their relative abundance from Cambrian to Devonian strata, prior to the Variscan (Upper Devonian–Lower Carboniferous) orogenic event that conforms the architectural grain of Western Europe. In addition, recent data from the rocks representing the most seaward part of the Paleozoic Iberian margin of Gondwana (Basal Units and Parautochthonous sequences) also provided evidence for the presence of Tonian–Stenian zircons (Díez Fernández et al. 2010, 2012; Dias da Silva 2013) although in a significantly lower proportion than in the allegedly coeval clastic rocks from the Central Iberian, West Asturian Leonese and Cantabrian zones (Fig. 1) of NW Iberia (see below).

The large volume of isotopic data (namely U–Pb detrital zircon ages and whole rock Sm–Nd isotopes) from Ediacaran and especially Paleozoic rocks from the northern Gondwanan realm published in the past decade has provided new arguments to revisit and reconsider the aforementioned ideas.

Furthermore, geochronological and isotopic work carried out on the terranes exposed in northern Africa, the Arabian peninsula and Iran in the last decade has shown the existence of significant amounts of Tonian–Stenian detrital zircons in some of the Paleozoic clastic sequences (Avigad et al. 2003, 2007, 2012; Kolodner et al. 2006; Horton et al. 2008; Ramos et al. 2008; Meinhold et al. 2011; Cox et al. 2012; Williams et al. 2012; Altumi et al. 2013). The presence of ca. 1.0 Ga zircons in the Paleozoic sedimentary rocks of northeastern Africa and the Arabian Nubian Shield (ANS) and also the Nd isotope systematics of these clastic rocks have led some authors (e.g., Gómez Barreiro et al. 2007; Bea et al. 2010; Díez Fernández et al. 2010, 2012) to suggest that NW Iberia was located in a more easterly position than that proposed by Fernández-Suárez et al. (2000, 2002a, b) and Gutiérrez-Alonso et al. (2003) and implicitly argue against the juxtaposition of an Amazonia-derived terrane against the African northern margin of Gondwana.

In addition, available data (e.g., Wilde and Youssef 2002; Avigad et al. 2007, 2012; Horton et al. 2008; Abati et al. 2010; Linnemann et al. 2011; Meinhold et al. 2011; Cox et al. 2012) indicate that Ediacaran rocks in northern Africa are devoid or contain scarce Tonian–Stenian zircons, except in the Sinai desert (Be'eri-Shlevin et al. 2009). Given that most Ediacaran samples in northern Africa have provided significantly fewer Tonian–Stenian zircons than their counterparts in NW Iberia, it is difficult to make straightforward inferences about the paleoposition of Iberia during Ediacaran times and about its correlation with the putative sources available in northern Africa at the time the Iberian Ediacaran sequences were deposited.

Recent work both in northern Africa and in the peri-Gondwanan terranes of Europe has focused on the Paleozoic sequences and generated a large database of detrital zircon U–Pb ages from clastic sedimentary rocks ranging in age from Middle Cambrian to Carboniferous. We feel that the currently available database of detrital zircon ages for Ediacaran and early Cambrian rocks in NW Iberia relies mostly on the works of Fernández-Suárez et al. (2000) and Gutiérrez-Alonso et al. (2003), which do not report a sufficient number of analyses to be statistically representative based on current practice in the study of detrital zircon age populations (e.g., Vermeesch 2012).

In this study, we present 1,161 new U–Pb ages of detrital zircons from four Ediacaran and two Lower

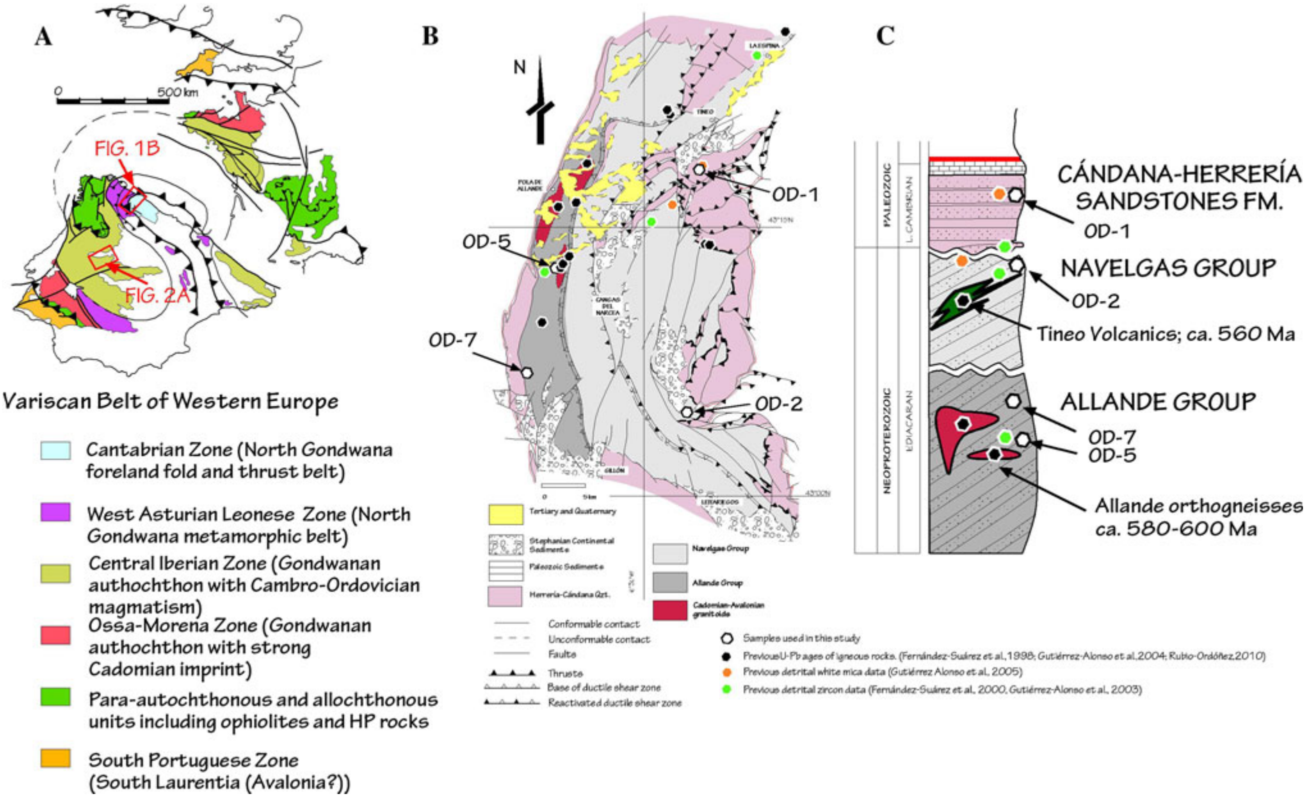

Fig. 1 **a** Variscan Belt of Western Europe depicting the oroclines present in Iberia (modified from Martínez Catalán 2012; Shaw et al. 2012a, b); **b** geological map including sample locations; **c** simplified stratigraphic column for the Narcea Antiform

Cambrian clastic sedimentary rocks of NW Iberia, which constitute a statistically robust database upon which to further investigate both the possible paleogeographic scenarios for Iberia in Ediacaran–Early Cambrian times (ca. 630–530 Ma) and the subsequent Paleozoic evolution.

Geological setting

Northwest Iberia exposes one of the most complete sections of the Ediacaran succession as well as an almost complete Paleozoic passive margin sequence deposited on the northern margin of Gondwana (Fig. 1). In this region, Ediacaran and Paleozoic strata lie within the tightly curved core of the Late Paleozoic Iberian–Armorican Arc (Fig. 1). If this arc, together with its continuation, the Central Iberian Arc (Martínez Catalán 2011; Martínez Catalán 2012; Shaw et al. 2012a, b), is restored to its pre-Variscan geometry (Weil et al. 2001, 2010, 2013a, b), the Iberian continental platform of Gondwana is shown to be very extensive (in excess of 2,000 km in length) and located adjacent to West Africa along the southern flank of the Rheic Ocean throughout the Paleozoic (Robardet 2002, 2003; Martínez Catalán et al. 2007; Nance et al. 2010).

The Iberian Massif is traditionally divided into zones based mainly on the differences in their Lower Paleozoic sedimentary successions, which are interpreted to reflect their relative proximity to the Gondwanan margin (Fig. 1). From the ancient coastline seaward toward the Gondwanan outer platform, five such zones are identified. The Cantabrian Zone (CZ) preserves a coastal environment and constitutes the Late Paleozoic foreland fold and thrust belt of the Iberian Variscan Belt (IVB), whereas the West Asturian Leonese (WALZ), Central Iberian (CIZ) and Galicia-Tras-os-Montes (Schistose Domain) zones, together with the Ossa-Morena Zone of southern Iberia, preserve a more outboard tectonostratigraphy (Julivert et al. 1972; Quesada 1990; Ribeiro et al. 1990; Pérez-Estaún et al. 1991; Quesada et al. 1991; Martínez-Catalán et al. 1997; Gutiérrez-Marco et al. 1999; Marcos and Farias 1999; Martínez Catalán et al. 1999; Aramburu et al. 2002; Robardet 2002, 2003; Robardet and Gutiérrez-Marco 1990) and contain the geological record of the orogenic hinterland. Boundaries between these zones are major Variscan thrusts and reverse faults that were, in some cases, reactivated by extension in the aftermath of the Variscan Orogeny (Martínez-Catalán et al. 1997; Martínez Catalán et al. 2003).

Late Paleozoic closure of the Rheic Ocean is recorded in northwest Iberia by the deformation associated with the Laurussia–Gondwana collision, the Variscan Orogeny, and in the oceanic remnants preserved as ophiolites in the allochthonous units of NW Iberia representing the rootless suture between these continents (e.g., Sánchez Martínez et al. 2009 and references therein; Fig. 1).

Within this tectonic framework, the Ediacaran and Early Cambrian rocks of Iberia crop out extensively throughout the western IVB and their origin and significance have been a subject of debate for decades. The succession is very homogeneous and dominated by siliciclastic rocks of uncertain thickness with some intercalations of minor limestone and volcanic rocks, which can be locally abundant.

Ediacaran strata crop out in the Cantabrian and West Asturian Leonese zones in two arcuate-shaped exposures, structured as large antiforms known as the Villalba and Narcea antiforms (Martínez Catalán 1985; Gutiérrez-Alonso 1996), the latter being better understood owing to its low to very low metamorphic grade and the detailed work performed on it (Gutiérrez-Alonso 1996; Gutiérrez-Alonso and Nieto 1996; Díaz García 2006; Abad et al. 2003; Rubio-Ordóñez 2010; Pastor-Galán et al. 2009 and 2012a).

The exposed Ediacaran sequence in the Narcea Antiform Domain has been variously known as the Narcea Slates or Mora Formation (de Sitter 1961) and interpreted as a thick continuous sequence of turbidites. Recently, this sequence was subdivided into two different stratigraphic units (Rubio-Ordóñez 2010, in press) based on igneous rock content and geochronological constraints. These two units are bound by complex thrust systems and shear zones (Gutiérrez-Alonso 1996). The lower part of the sequence, cropping out to the west of the Narcea Antiform, is known as the Allande Unit and is composed of sandy and pelitic rocks with abundant interbedded volcanic and volcanoclastic rocks up to 3 km thick. This sequence is intruded by several bodies of decametric to kilometric Ediacaran granites, granodiorites and gabbros whose intrusion ages range from ca. 580 to 590 Ma (Fernández-Suárez et al. 1998; Rubio-Ordóñez et al. in press), providing a constraint on their minimum depositional age. Overlying both the Allande Unit and the Ediacaran intrusive rocks, there is another siliciclastic sequence known as the Navelgas Unit, containing scarce interbedded andesitic volcanic complexes with thicknesses up to ca. 1 km which have been dated at ca. 560 Ma (Gutiérrez-Alonso et al. 2004; Rubio-Ordóñez 2010, in press).

The Ediacaran succession in the Central Iberian Zone (CIZ) of central Iberia (Fig. 2) and especially in the study area comprises a lowermost thick siliciclastic (with scarce carbonate beds and volcanics) unit known as Schist and Greywacke Complex (SGC) (Carrington da Costa 1950). The uppermost parts of this sequence are lower Cambrian in age. This sedimentary succession has been subdivided into different units (Fig. 2b) by several authors, and the following are the Ediacaran parts of the succession: Lower Unit and the lower part of the Upper Unit (Rodríguez Alonso 1985; Rodríguez-Alonso et al. 2004); the lower part of the Monterrubio Formation (Díez Balda 1986); and units

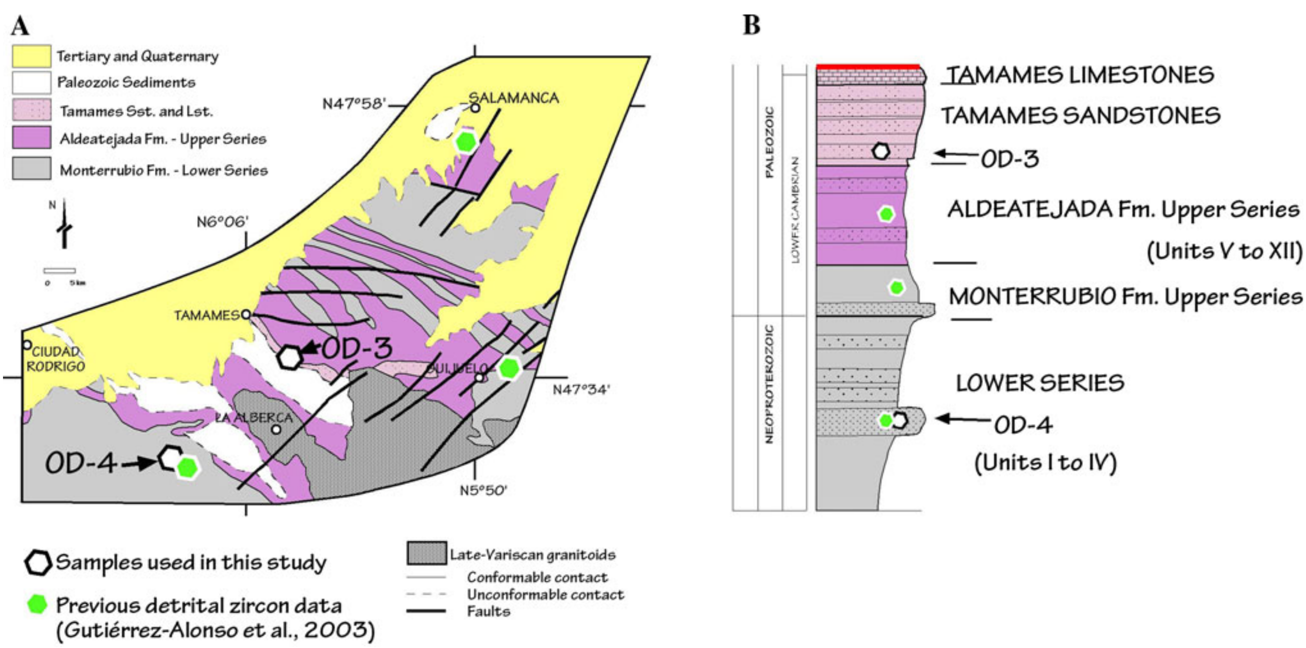

Fig. 2 **a** Geological map, sample location and **b** simplified stratigraphic column for the Central Iberian Zone

I–IV (Valladares et al. 1998, 2000, 2002) which are indicated in Fig. 2b. The age of these sequences is uppermost Ediacaran (Vendian) (Vidal et al. 1994) based on their microfossil content.

There is no general consensus on the origin and tectonic setting of the mainly turbiditic rocks that constitute the Ediacaran sequence in the Central Iberian Zone. Several authors consider them to represent a passive margin sequence (Valladares 1995; Valladares et al. 1998, 2000, 2002, 2006; Ugidos et al. 1997a, b, 2003a, b) sharing a common source (Ugidos et al. 2010). Other authors favor the origin of these rocks in a subduction-related environment as peri-arc sediments (Fernández-Suárez et al. 1998, 2000, 2002a, b; Gutiérrez-Alonso et al. 2003; Rodríguez-Alonso et al. 2004; Rubio-Ordóñez 2010; Pereira et al. 2012b; Rubio-Ordóñez et al. in press).

The Lower Cambrian succession shows different characteristics from northern to central Iberia. In the Narcea Antiform (northern section), it lays unconformably on the top of the previously deformed Allande and Navelgas Units (de Sitter 1961; Julivert and Martínez García 1967; Angerer 2007). This unconformity is indicative of a tectonic event close to the Ediacaran–Cambrian boundary, although the extent and nature of this deformation are not yet fully characterized (e.g., Gutiérrez-Alonso 1996; Díaz García 2006). The lower Cambrian rocks in NW Iberia and the Cándana–Herrería Formation consist mainly of a ca. 1,000–1,500-m-thick succession of feldspathic sandstone, quartzite, shale and distinct conglomerates and dolomite layers near or at the base of the sequence. The conglomerate rocks contain pebbles derived from the Navelgas Unit volcanic rocks (Rubio-Ordóñez et al. 2004, in press). In contrast with the underlying Ediacaran rocks, the Cándana–Herrería Formation is interpreted to be deposited in a braid plain delta environment (Aramburu et al. 1992, 2002), and paleontological studies have provided a Lower Cambrian depositional age (Palacios and Vidal 1992; Vidal et al. 1994, 1999; Gozalo et al. 2003). Previous detrital zircon (Fernández-Suárez et al. 2000) and white mica (Gutiérrez-Alonso et al. 2005) geochronological studies provided preliminary data on the provenance of this formation (see discussion below). Above the Cándana–Herrería Formation, there is a distinct carbonate formation (Láncara Formation) where the lower to middle Cambrian transition is found (Zamarreño 1972; Álvaro et al. 2000) in a low morphology carbonate ramp (Wotte 2009).

The Cambrian succession in the CIZ lays conformably over the Ediacaran deposits described above and is composed by the upper part of the SGC, the Tamames Sandstones and the Tamames Limestone (correlated with the Láncara Formation). The Cambrian rocks of the SGC have also been subdivided into different units (Fig. 2b) by several authors as follows: Cambrian strata comprise the highest part of the Upper Unit (Rodríguez Alonso 1985; Rodríguez-Alonso et al. 2004); part of the Monterrubio and Aldeatejada formations (Díez Balda 1986); and units V to XII (Valladares et al. 1998, 2000, 2002) which are indicated in Fig. 2b. A lowermost Cambrian age is attributed to this succession based mostly on the presence of acritarchs, trilobites and ichnofossils (Vidal et al. 1994, 1999; Gozalo et al. 2003; Jensen et al. 2010). Although its depositional environment is debated, this succession is generally interpreted to represent platform deposits. There is evidence of syn-sedimentary tectonic activity such as the presence of olistostromal deposits, mostly in strata deposited near the Ediacaran–Cambrian boundary (Rodríguez-Alonso et al. 2004). Conformably above the Cambrian SGC rocks, the lower Cambrian Tamames sandstone (Díez Balda 1986; Vidal et al. 1994) consists of a ca. 600-m-thick succession of shallow marine quartzitic sandstones deposited under subtidal conditions (Rodríguez Alonso and Alonso Gavilán 1995).

Samples and methods

Samples

Six sandstone samples were collected for this study, and sample locations are given in the geological maps and in the synthetic stratigraphic columns of Figs. 1 and 2. Samples are described below in ascending stratigraphic order.

Samples OD5 (43°11′55.37″N; 6°36′02.50″W) and OD7 (43°06′31.08″N; 6°38′26.05″W) are medium and fine-grained sandstones with abundant plagioclase and deformed under low-grade metamorphic conditions (Fig. 3) from the Ediacaran Allande Unit in the Narcea Antiform. OD5 was collected close (ca. 300 m) to the intrusive contact with the ca. 590 Ma Puente de Selce granitoid body (Fernández-Suárez et al. 1998) although no contact metamorphism effects are visible in the studied sample, and OD7 was collected along strike in the same unit away from the intrusive rocks. This sample is equivalent to sample JG-12 of Fernández-Suárez et al. (2000).

Sample OD2 (43° 6′26.80″N; 06°26′52.01″W) is a fine-grained sandstone (Fig. 3) from the uppermost Ediacaran Navelgas Unit near the eastern boundary of the Narcea Antiform, where the metamorphic grade is very low (Gutiérrez-Alonso and Nieto 1996; Pastor-Galán et al. 2009). This sample can be correlated with samples JG-1 and SJ-1 of Fernández-Suárez et al. (2000) in the nearby Villalba Antiform and with sample ZD-3 of Gutiérrez-Alonso et al. (2003) in the Narcea Antiform. This sample is also correlated with the sample MD-1 of Gutiérrez-Alonso et al. (2005) which provided $^{40}Ar/^{39}Ar$ ages of detrital micas ranging from ca. 590 to 783 Ma (Fig. 1c).

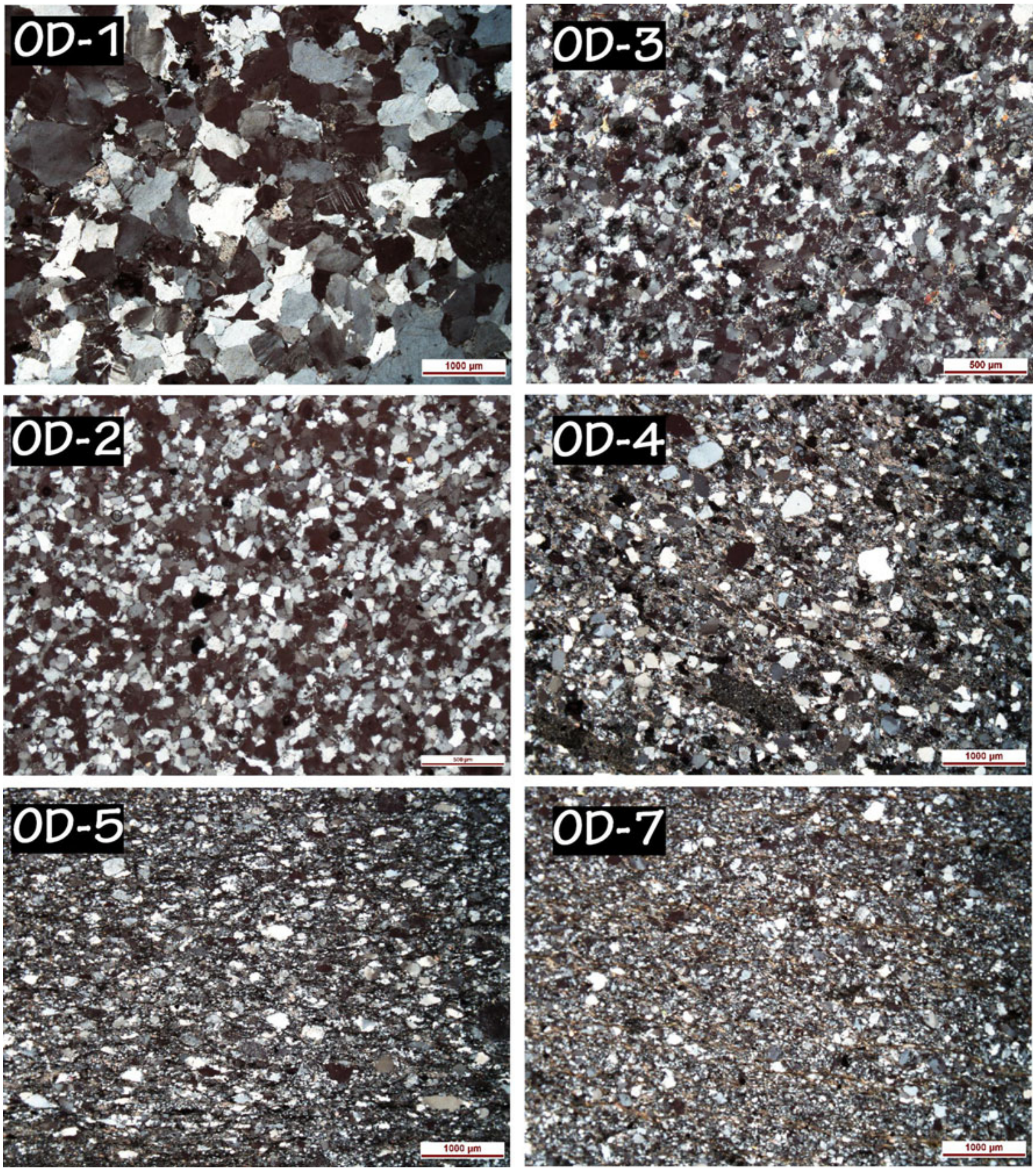

Fig. 3 Photomicrographs of the studied samples

Sample OD4 (40°25′39.25″N; 06°16′36.85″W) was collected in the Ediacaran rocks of the Central Iberian Zone, in the Lower Unit (Rodríguez Alonso and Alonso Gavilán 1995) or Serie II (Valladares et al. 2000, 2002). The sample was taken from a coarse-grained sandstone layer (Fig. 3) interbedded within a predominantly conglomeratic unit. This sample is equivalent to sample ZD-2 of Gutiérrez-Alonso et al. (2003) and both were collected in the same outcrop (Fig. 2b).

Sample OD3 (40°36′25.93″N; 6°02′07.85″W) is a medium-grained shallow marine sandstone (Fig. 3) from the lower Cambrian Tamames Formation in the Central Iberian Zone and was collected in the type locality of *La Rinconada*, where this formation has been dated with fossils and ichnofossils (Díez Balda 1986). Samples ZD-4 and ZD-1 in Gutiérrez-Alonso et al. (2003) were collected in the underlying lower Cambrian part of the SGC (see above and Fig. 2b).

Sample OD1 (43°17′43.79″N; 6°25′56.04″W) corresponds to coarse, feldspar-rich coastal to shallow marine quartzite (Fig. 3) from the unmetamorphosed Lower Cambrian Cándana–Herrería Formation in the Cantabrian Zone. Sample JG-16 in Fernández-Suárez et al. (2000) was also collected within this formation (Fig. 1c) but cannot be considered as a temporal equivalent to OD1 as it was collected just a few meters above the angular unconformity with the Navelgas Unit (see Fig. 1c) and there is a considerable probability that the zircons contained in sample JG-16 could be recycled from the underlying Ediacaran rocks. Sample OD1 was collected at the same locality as sample MD-2 (Gutiérrez-Alonso et al. 2005) which yielded 3 different groups of $^{40}Ar/^{39}Ar$ detrital, single grain, white mica ages: 550–650; 950–1,050; and 1,600–1,800 Ma.

Geochemistry

All studied samples were analyzed for major and trace elements and rare earth elements (REE) (Table 1 in electronic online supplement). The samples were analyzed by X-ray fluorescence using a Philips PW2400 X-Ray spectrometer for major and selected trace (Rb, Sr, Ba, Zr, Nb, Y, Zn, V, Cr and Ni) elements in the Nova Scotia Regional Geochemical Centre at Saint Mary's University, Canada. Details of analytical methods as well as precision and accuracy of the X-ray data are reported by Dostal et al. (1994).

Samples were analyzed for REE and additional trace element (Hf, Ta and Th) abundances at Memorial University (Newfoundland) by inductively coupled plasma-mass spectrometry according to the methods described by Longerich et al. (1990).

Sm–Nd isotopic analyses were performed at the Atlantic Universities Regional Isotopic Facility at Memorial University on a Finnigan MAT 262V TI-mass spectrometer in static mode. Further information on Sm–Nd analytical procedures is given in Kerr et al. (1995). Nd isotopic ratios are normalized to $^{146}Nd/^{144}Nd = 0.7219$. The reported values were adjusted to La Jolla Nd standard ($^{143}Nd/^{144}Nd = 0.511860$). During the course of data acquisition, replicates of the standard gave a mean value of $^{143}Nd/^{144}Nd = 0.511888 \pm 16$ (2σ, $n = 12$). The in-run precision on Nd isotopic ratios is given at 95 % confidence level. Errors on Nd isotopic compositions are <0.002 %, and errors on the $^{147}Sm/^{144}Nd$ ratio are estimated to be less than 0.1 %.

The ε_{Nd} values (Table 2 in electronic online supplement) were calculated using a $^{143}Nd/^{144}Nd = 0.512638$ value for the present-day chondrite uniform reservoir (CHUR). ^{147}Sm decay constant is 6.54 10^{-12} year^{-1} (Steiger and Jäger 1977). T_{DM} values (Table 2 in electronic online supplement) were calculated with respect to the DePaolo mantle model (DePaolo 1981, 1988) for the depositional age of the studied rocks.

U–Pb analytical method

Samples were crushed with a jaw crusher and pulverized with a disc mill. Zircons were separated at the Salamanca and Complutense (Madrid) Universities by heavy fraction enrichment on a Wilfley table followed by density separation using di-iodomethane (CH_2I_2) and magnetic separation in a Frantz isodynamic separator. Zircons were selected from the least magnetic fraction and hand-picked in alcohol under a binocular microscope. Zircon grains were set in synthetic resin mounts, polished to approximately half their thickness and cleaned in a warm HNO_3 ultrasonic bath.

Zircons were analyzed for U and Pb isotopes by LA–ICP–MS at the Museum für Mineralogie and Geologie (Senckenberg Naturhistorische Sammlungen Dresden), using a Thermo-Scientific Element 2 XR sector field ICP–MS coupled to a New Wave UP-193 Excimer Laser System. Further details on the analytical protocol and data reduction are given in Frei and Gerdes (2009).

U–Pb data treatment and presentation

A total of 240 U–Pb age determinations were performed on each sample (one analysis in the center of each grain). After data reduction and age calculation, analyses with discordance higher than 10 % (i.e., concordance <90 or >110 %) were rejected. The number of non-rejected analyses ($n > 120$ per sample) makes it unlikely that any fraction of the age populations comprising more than 0.05 % of the total is overlooked at the 95 % confidence level (Vermeesch 2004). The U–Pb data are given in Tables 3–8 (electronic online supplement) and represented for visualization and comparison in the Concordia plots of Fig. 5 and the Kernel density estimation plots (KDE plots henceforth) of Fig. 6. These graphs were drawn using *Isoplot 3.7* (Ludwig 2009) and *Density Plotter v1.4* (Vermeesch 2012), respectively. The KDE graphs of Fig. 6 also show the corresponding probability density plots (PDD) constructed using the *AgeDisplay* program (Sircombe 2004). Age assignment to each analysis (*Reported Age* column in Tables 3–8 in electronic online supplement) is as follows: For analyses whose 2σ error ellipse overlaps the concordia curve, the chosen age and 2σ uncertainty are the *Concordia age* and error (Ludwig 1998) as calculated by *Isoplot 3.7* (Ludwig 2009). For analyses that are less than 10 % discordant but whose corresponding 2σ ellipses do not intercept the concordia curve, we have chosen either the $^{207}Pb/^{206}Pb$ or the $^{206}Pb/^{238}U$ age depending on which corresponding isotope ratio was measured with more precision in that particular analysis.

Maximum sedimentation age for each sample was calculated as the weighted average of the $^{206}Pb/^{238}U$ age of the youngest (concordant) grains whose corresponding ellipses overlap at 2σ (Fig. 6) (see ad hoc discussion in Dickinson and Gehrels 2009).

Comparison of age distributions (Fig. 7a) between samples was made using a Kolmogorov–Smirnov nonparametric test (whether two independent samples have been drawn from the same—unspecified—parent population) in a similar way as it has been used in previous studies to establish common provenance (DeGraaff-Surpless et al. 2003; Amidon et al. 2005; Dickinson et al. 2009, 2010; Barbeau et al. 2009). In the present context, any two samples that pass the test (see below) can be regarded as derived from erosion of the same source area, or at least from source areas whose rocks contain the same parent zircon populations in virtually the same relative proportions. This test was performed using the program *OriginPro 9.0* using the *Reported Age* data in Tables 3–8 (electronic online supplement) (or similarly constructed data tables in the case of data taken from previous studies).

The cumulative fraction plots of Figs. 7b and 8 were constructed using the software available online at http://www.physics.csbsju.edu/stats/KS-test.html.

Lithogeochemistry and Sm–Nd isotope results

The lithogeochemical data (Tables 1, 2 in electronic online supplement) plotted on a variety sediment geochemical discrimination diagrams are shown in Fig. 4. With the exception of sample (OD1), all rocks have major and trace element geochemistry consistent with an active continental margin to continental island arc setting. Sample OD1, on the other hand, has significantly lower FeO, MgO, TiO_2 and significantly higher SiO_2, and has a composition akin to that of sedimentary rocks of passive margin settings. The environments inferred from these diagrams are in agreement with regional syntheses based on a wealth of geochemical data from igneous rocks that this portion of the Gondwanan margin underwent a transition from a continental arc in the Ediacaran to a passive margin in the early Cambrian (e.g., Nance et al. 2008 and references therein).

Sample OD1 has significantly lower ΣREE, but higher La/Sm compared to the other samples, suggesting fractionation of some accessory minerals during sediment transport. All samples display a negative Eu anomaly, suggesting derivation from either (1) a crustal source that was fractionated with respect to feldspar or (2) chemical weathering of feldspar at the source or during transport.

The Nd isotopic signature in clastic rocks represents the weighted average of the detrital contributions from the various source areas (e.g., Murphy and Nance 2002). The

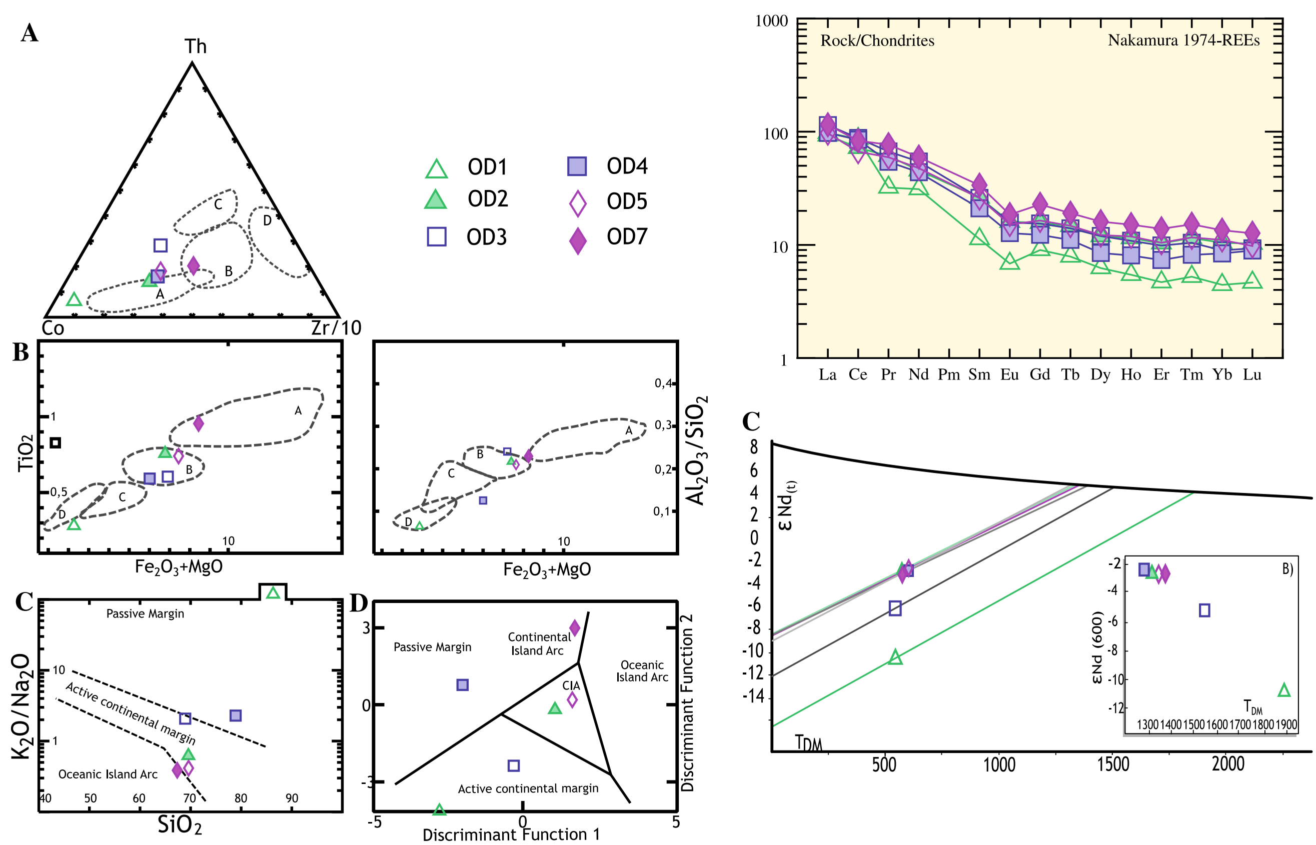

Fig. 4 Relevant Geochemical plots for samples OD1, OD2, OD3, OD4, OD5 and OD7 (see text for details). **a** Major and trace element-based discrimination diagrams; **b** chondrite normalized REE plot; **c** $\varepsilon_{(Nd)}$ versus time plots. Initial $\varepsilon_{(Nd)}$ calculated for the stratigraphic age (see also Fig. 6). T_{DM} values calculated according to the DePaolo (1981) depleted mantle model

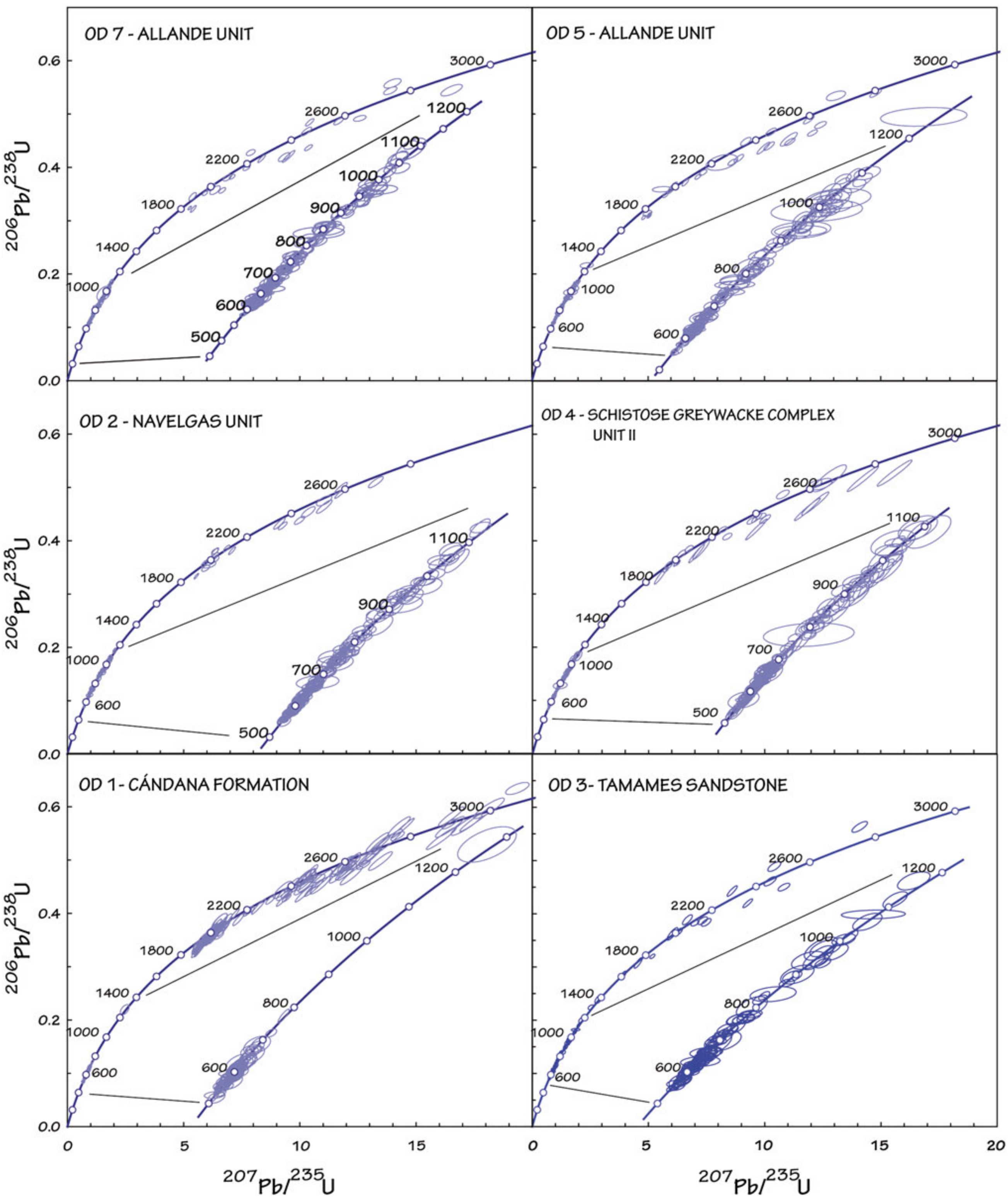

Fig. 5 U–Pb Concordia plots for samples OD1, OD2, OD3, OD4, OD5 and OD7. *Ellipses* represent 2 sigma uncertainties

difference between OD1 and the other samples is also clear from the Sm–Nd isotopic data (Fig. 4), which indicates that the Cambrian sample has significantly lower $\varepsilon_{Nd(i)}$ (−11.0) and higher T_{DM} (ca. 1.9 Ga) compared to the other Ediacaran and Cambrian sedimentary rocks. Although not as pronounced, Cambrian sample OD3 also has lower $\varepsilon_{Nd(i)}$

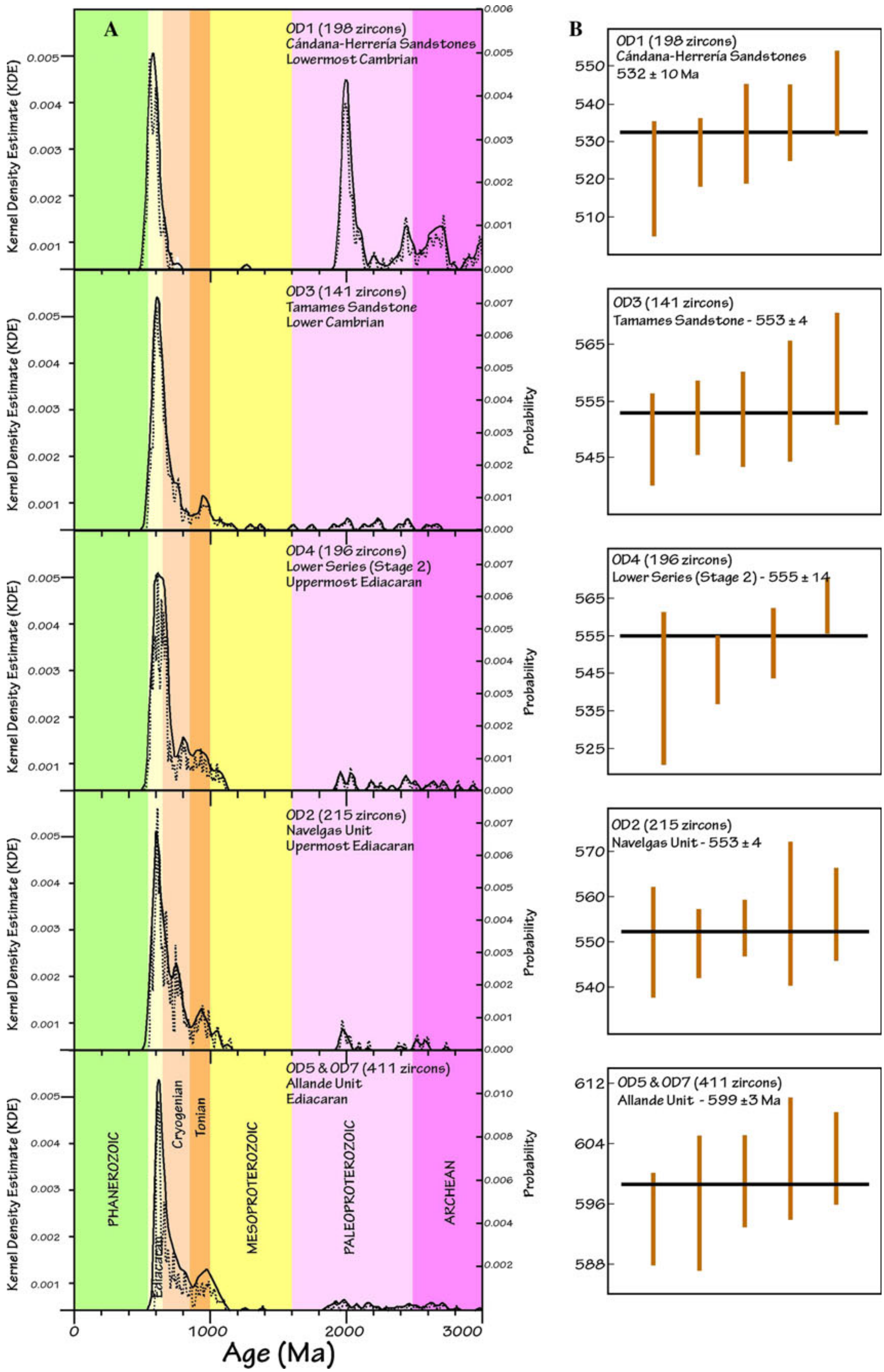
A
OD1 (198 zircons)
Cándana-Herrería Sandstones
Lowermost Cambrian
OD3 (141 zircons)
Tamames Sandstone
Lower Cambrian
OD4 (196 zircons)
Lower Series (Stage 2)
Uppermost Ediacaran
OD2 (215 zircons)
Navelgas Unit
Upermost Ediacaran
OD5 & OD7 (411 zircons)
Allande Unit
Ediacaran
Kernel Density Estimate (KDE)
Probability
PHANEROZOIC
Ediacaran
Cryogenian
Tonian
MESOPROTEROZOIC
PALEOPROTEROZOIC
ARCHEAN
Age (Ma)
B
OD1 (198 zircons)
Cándana-Herrería Sandstones
532 ± 10 Ma
OD3 (141 zircons)
Tamames Sandstone - 553 ± 4
OD4 (196 zircons)
Lower Series (Stage 2) - 555 ± 14
OD2 (215 zircons)
Navelgas Unit - 553 ± 4
OD5 & OD7 (411 zircons)
Allande Unit - 599 ±3 Ma

◀**Fig. 6** **a** Kernel density estimation plots for samples OD1, OD2, OD3, OD4, OD5 and OD7. In all plots the wavelength (h) is 20 Myr (*Black line* is KDE calculated using Density Plotter 1.4 of Vermeesch 2012). *Dashed line* is the probability density plot calculated using the Age Display software (Sircombe 2004); **b** maximum depositional age calculated as described in main text (analytical methods)

(−6.0) and higher T_{DM} (ca. 1.6 Ga) compared to the Ediacaran rocks. All other samples analyzed have very similar $\varepsilon_{Nd(i)}$ (–2.0 to −3.0) and T_{DM} (ca. 1.3–1.4 Ga).

U–Pb results

The Allande Unit

Both OD5 and OD7 samples are from Allande Unit which is Ediacaran in age (Rubio-Ordóñez 2010) (see above). A Kolmogorov–Smirnov test (KS test henceforth) indicates that the U–Pb age distributions in these two samples are not significantly different at the 5 % confidence level (Fig. 7), and therefore, we have combined the U–Pb data from these two samples ($n = 411$) in the following discussion as well as in the graphs of Figs. 6 and 8.

Based on the dataset of combined OD5 and OD7 samples, the Allande Unit (Tables 7 and 8 in electronic online supplement, Fig. 5) has a maximum sedimentation age of 599 ± 3 Ma (Fig. 6). As these strata are intruded by ca. 580–590 Ma, I-type calc-alkaline granitoids (Fernández-Suárez et al. 1998; Rubio-Ordóñez et al. in press), the depositional age of Allande Unit is constrained between ca. 600 Ma and 580 Ma. The combined OD5 and OD7 samples show the following distribution of detrital zircon ages: Ediacaran (time scale according to International Commission on Stratigraphy, 2012) zircons are 25 % of the total data ($n = 411$). Cryogenian zircons (630–850 Ma) are 44 % of the total population. Tonian (850–1,000 Ma) zircons are 13 % of the total population, and Mesoproterozoic (Stenian) zircons (1–1.2 Ga) are 6 % of the data. Paleoproterozoic zircons are 8 % of the population, and Archean zircons are 4 % of the population. A total of 82 % of zircons are of Neoproterozoic age, and almost all the Mesoproterozoic zircons (with two exceptions) are younger than 1.1 Ga. The distribution of U–Pb ages in Paleoproterozoic zircons (from ca. 1.85 to 2.45 Ga) does not show clear maxima, and the Archean zircon ages are mostly comprised between ca. 2.5 and 2.8 Ga.

The Navelgas Unit

The detrital zircon data for sample OD2 (Table 4 in electronic online supplement, Figs. 5, 6) yield a maximum sedimentation age of 553 ± 4 Ma as well as the following age distribution: Ediacaran zircons are 35 % of the total data ($n = 215$). Cryogenian zircons are 40 % of the total population. Tonian zircons are 12 % of the total population, Mesoproterozoic (Stenian) zircons are 4 %, Paleoproterozoic zircons are 6 % of the population, and Archean zircons are 3 % of the population. A total of 87 % of zircons are of Neoproterozoic age, and all the Mesoproterozoic zircons are younger than 1.2 Ga.

Schist and Greywacke complex

The detrital zircon data for sample OD4 (Table 6 in electronic online supplement; Figs. 5, 6) yield a maximum sedimentation age of 555 ± 14 Ma and the following age distribution: Ediacaran zircons are 31 % of the total data ($n = 196$). Cryogenian zircons are 40 % of the total population. Tonian zircons are 11 % of the total population, Mesoproterozoic (Stenian) zircons are 5 %, Paleoproterozoic zircons are 8 % of the population, and Archean zircons are 5 % of the population. A total of 82 % of zircons are of Neoproterozoic age, and all the Mesoproterozoic zircons are younger than 1.2 Ga.

The Cándana–Herrería Formation

The detrital zircon data for sample OD1 (Table 3 in electronic online supplement; Figs. 5, 6) yield a maximum sedimentation age of 532 ± 10 Ma and the following age distribution: Cambrian zircons are 2 % of the total data ($n = 198$), Ediacaran zircons are 31 %, Cryogenian zircons are 6 %, Tonian zircons are absent, at variance with all other samples analyzed for this study, and only one Mesoproterozoic zircon was analyzed (1,273 ± 38 Ma). Paleoproterozoic zircons are 43 % of the population, and Archean zircons are 18 % of the population. Note that Paleoproterozoic and Archean zircons are 61 % of the population at extreme variance with all other samples where Neoproterozoic zircons are more than 80 % of the population.

The Tamames Formation

The detrital zircon data for sample OD3 (Table 5 in electronic online supplement; Figs. 5, 6) yield a maximum sedimentation age of 553 ± 4 Ma and the following age distribution: Ediacaran zircons are 37 % of the total data ($n = 141$). Cryogenian zircons are 38 % of the total population. Tonian zircons are 8 % of the total population, and Mesoproterozoic (Stenian) zircons are 5 %. Two older Mesoproterozoic zircons were analyzed, with ages of 1,299 and 1,375 Ma. Paleoproterozoic zircons are 9 % of the population, and Archean zircons are 3 % of the population. A total of 83 % of zircons are of Neoproterozoic age, and all the Mesoproterozoic zircons (with two exceptions) are younger than 1.2 Ga.

A Kolgomorov-Smirnov Test

Not significantly different (green) | Likely very similar (white) | Significantly different (red)

at the 0.05 significance level the sutidied populatins are: Red shaded cells have P<0.001, orange shaded cells have 0.05>P>0.001, green cells have P>0.05

P Value (upper right) / D Value (lower left)

	OD5	OD7	Combined OD7-OD5	OD2	OD4	OD3	OD1	Basal Units	Para-authochtonous (2)	Morocco Lower Cambrian (3)	Morocco Middle Cambrian (3)	Sardinia Cambrian (3)	CIZ - Portugal Ediacaran (4)	ANS (5)	Morocco Ediacaran (6)	Lybia Cambrian (7)
OD5		0.060		0.318	0.549	0.099	1.5E-30									
OD7	0.128			0.080	0.381	0.286	1.9E-32									
Combined OD7-OD5				0.601	0.529	0.442	2.3E-39	4.0E-35	9.9E-19				0.01295	0.20726		
OD2	0.095	0.124	0.065		0.825	0.297	6.8E-20	2.2E-16	4.3E-11		9.1E-4		0.02264	0.05998	1.3E-6	
OD4	0.080	0.089	0.071	0.058		0.443	1.9E-20	1.3E-12	2.6E-8		0.01056		0.00532	0.26959		
OD3	0.137	0.107	0.085	0.102	0.091		3.8E-19	4.3E-10	6.2E-7		6.5E-5	1.6E-10		0.03139		
OD1	0.639	0.641	0.638	0.484	0.490	0.515				1.3E-13				1.7E-29	6.7E-12	
Basal Units (1)			0.347	0.318	0.290	0.297			0.409	2.7E-31	2.3E-11			2.4E-23		2.9E-15
Para-authochtonous (2)			0.254	0.272	0.243	0.252		0.042		4.7E-29	2.2E-5			4.4E-12		1.9E-12
Morocco Lower Cambrian (3)							0.396	0.512	0.494							
Morocco Middle Cambrian (3)				1.193	0.162	0.250		0.292	0.196					0.0138		
Sardinia Cambrian (3)						0.460								2.9E-7		
CIZ - Portugal Ediacaran (4)			0.180	0.179	0.210									0.07754		
ANS (5)			0.097	0.115	0.088	0.143	0.535	0.349	0.250		0.143	0.337	0.145			
Morocco Ediacaran (6)				0.255			0.364									
Lybia Cambrian (7)								0.271	0.247							

(1) Díez Fernández et al., 2010
(2) Díez Fernández et al., 2012
(3) Avigad et al., 2012
(4) Pereira et al., 2012a
(5) Kolodner et al. 2006
(6) Abati et al., 2010
(7) Altumi et al., 2013

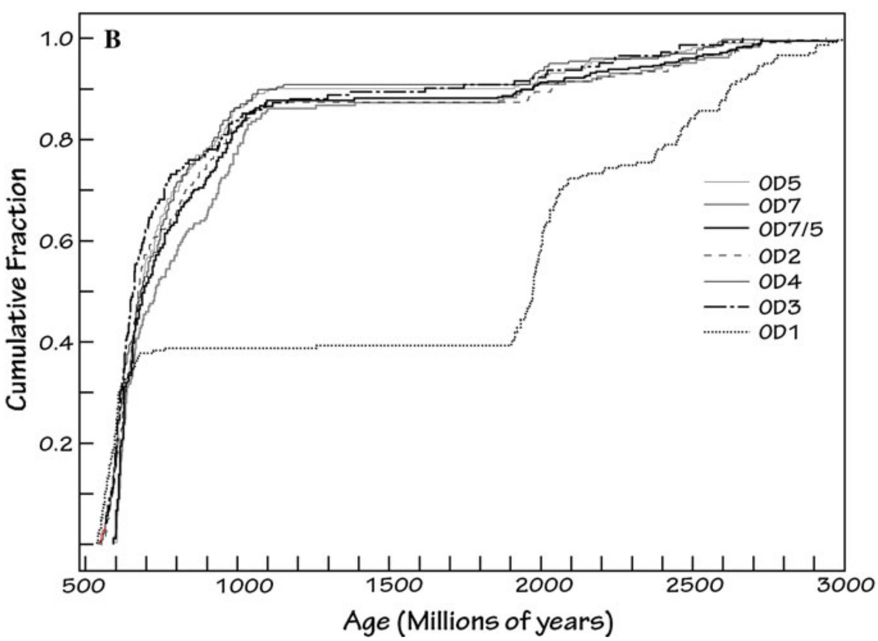

◀ **Fig. 7** **a** U–Pb age cumulative frequency plots. **b** Results of Kolmogorov–Smirnov test (see text for further information). The K–S test is a nonparametric test that compares cumulative probability curves to determine the likelihood (*P* value) that any two (age) curves can be obtained by random sampling of a single parent population (of unspecified distribution). If $P < 0.05$, there is a 95 % probability that the difference between the two tested populations is not due to random sampling error but rather indicates that these two samples are derived from different parent populations. *D* value represents the maximum distance between the cumulative frequency curves of the two tested populations. Strictly identical samples would have $P = 1$, $D = 0$

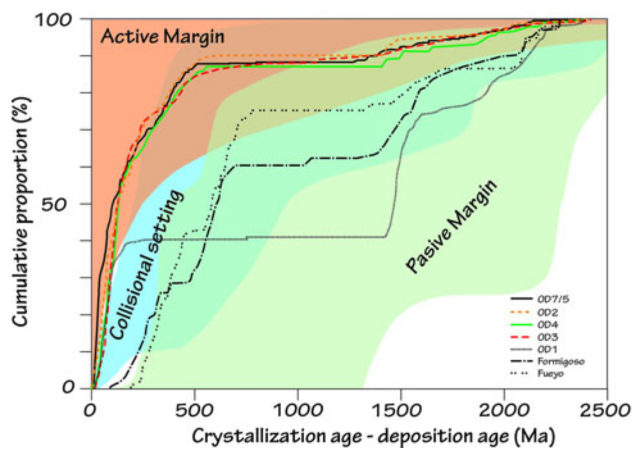

Fig. 8 CA–DA diagram of Cawood et al. (2012) showing the cumulative curves of samples OD1, OD2, OD3, OD4, OD5 and OD7. CA is the U–Pb age (Reported Age in Tables 3–8 in electronic online supplement) for each zircon. DA is the inferred depositional age of the rock unit in which the zircon was sampled. Note how all studied samples fall within the field of convergent margin settings

Discussion

Age and correlation of the Ediacaran and Cambrian formations

The data obtained on the Ediacaran–Cambrian formations in NW Iberia, combined with the available geological information, provide a more tightly constrained depositional framework and new insights into possible paleogeographic scenarios.

In the Narcea Antiform domain (Fig. 1), the lower part of the Ediacaran succession (Allande Unit) was deposited in a time interval bound by the age of the youngest group of detrital zircons (599 ± 3 Ma) (Fig. 6b) and the crystallization age of the granitoid bodies that intrude this unit (ca. 580–590 Ma, Fernández-Suárez et al. 1998). The Navelgas Unit, overlying the Allande Unit, has a maximum sedimentation age of 553 ± 4 Ma and contains volcanic intercalations dated at 559 ± 4 Ma (Gutiérrez-Alonso et al. 2004), and therefore, its depositional age is late Ediacaran. The KS test performed on samples OD5 and OD7 (Allande Unit) and OD2 (Navelgas Unit) indicates that the U–Pb age distributions are not significantly different (Fig. 7a, b). This observation is an indication that (1) both units are in stratigraphic continuity or separated by a minor unconformity and (2) the same source rocks were being eroded in the time interval between ca. 600 and 550 Ma. As sample OD2 (maximum depositional age ca. 553 Ma) contains a younger population (ca. 600–550) not present in OD5 or OD7, the data belonging to this younger age group were not used in the KS test.

Sample OD4 (SGC of the CIZ, Fig. 2) has a maximum depositional age of 555 ± 14, indistinguishable within error from that of sample OD2 (Navelgas Unit), and the KS test between samples OD4 and OD2 (Fig. 7a) indicates that the U–Pb age distributions are not significantly different. Based on these observations, the Navelgas Unit and the lower part of the SGC can be considered to be coeval with a late Ediacaran depositional age. Samples OD2 and OD4 correspond to locations that, if the Iberian oroclines are restored to an initial near lineal geometry (see above), could have been about 1,000 km apart in depositional time coordinates (Shaw et al. 2012a, b), providing an indication of the scale of the alongshore uniformity of detrital influx in late Ediacaran times.

Sample OD1 (Lower Cambrian) unconformably overlies the late Ediacaran Navelgas Unit and has a maximum depositional age of 532 ± 10 Ma (Fig. 6), consistent with its paleontologically constrained Early Cambrian age (see above). The zircon U–Pb age distribution in this sample is strikingly different to that of the underlying Ediacaran samples OD5, OD7 and OD2 (Figs. 6, 7) (see also U–Pb results section above). Furthermore, when applying a KS test to the 550–750 Ma U–Pb age interval of samples OD1 and OD2 (not shown in Fig. 7a), the two samples are significantly different in that interval, indicating a different source area, either local or remote, for the Early Cambrian rocks in the Cantabrian Zone, which adds to the first-order difference defined by the absence of a Tonian–Stenian population and high proportion of Paleoproterozoic zircons in sample OD1. The detrital zircon age distribution in sample OD1 with respect to samples OD5, OD7 and OD2 indicates that in Early Cambrian times, there was a first-order change in either the drainage system or the nature of the source area feeding the basin now recorded in the sedimentary succession of the Narcea Antiform domain.

Sample OD3 (Lower Cambrian Tamames Formation in the CIZ, Figs. 1, 2) has a maximum depositional age of 553 ± 4 Ma (Fig. 6) and in contrast with sample OD1 (Lower Cambrian in the Narcea Antiform Domain) does not contain any Paleozoic zircons. The Tamames Formation is in apparent stratigraphic continuity with the underlying SGC (OD4), and a KS test between these two samples shows that their detrital zircon U–Pb age

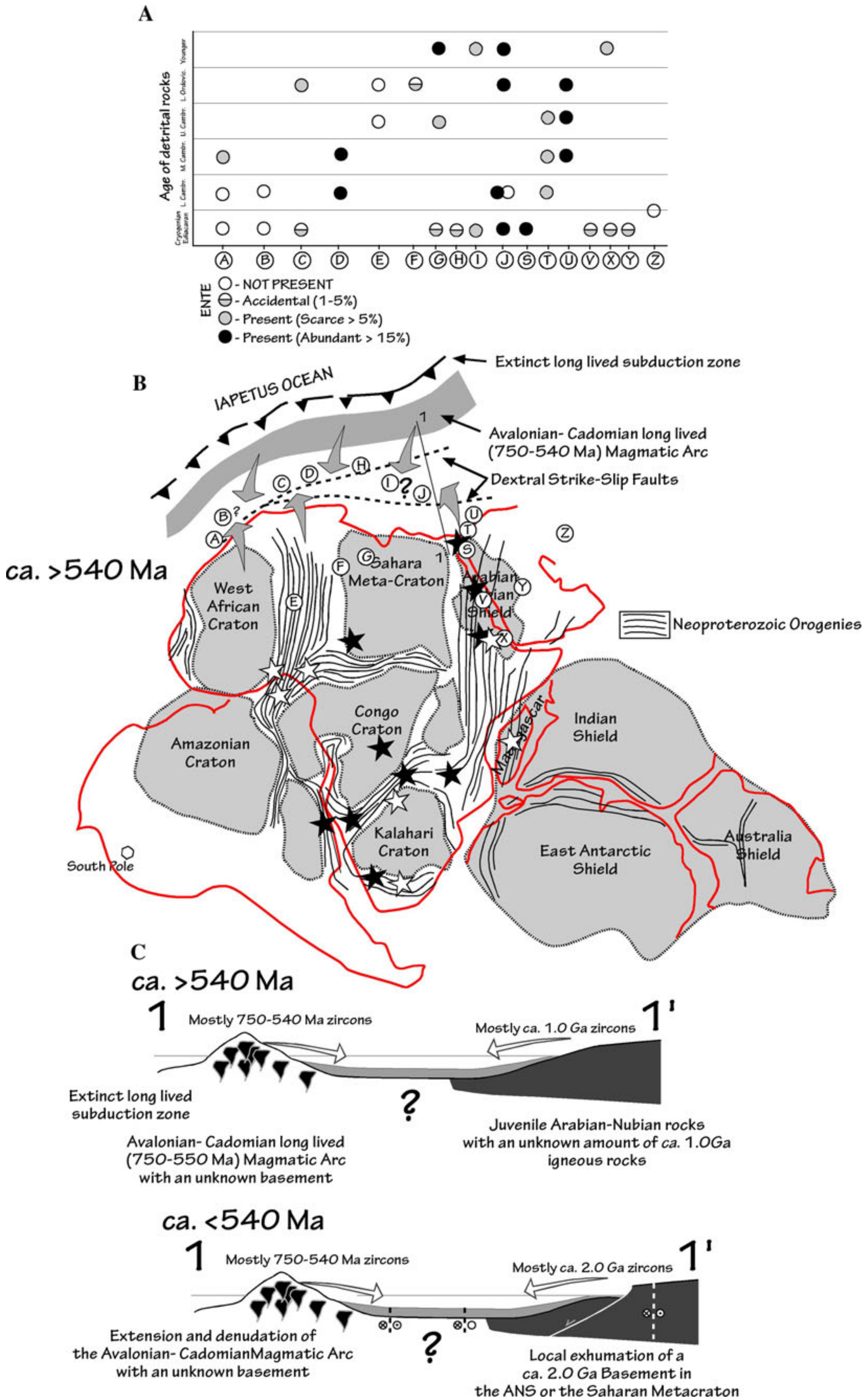
A
Age of detrital rocks
Younger
L. Ordovic.
U. Cambr.
M. Cambr.
L. Cambr.
Cryogenian Ediacaran
A B C D E F G H I J S T U V X Y Z
ENTE
- NOT PRESENT
- Accidental (1-5%)
- Present (Scarce > 5%)
- Present (Abundant > 15%)
B
IAPETUS OCEAN
Extinct long lived subduction zone
Avalonian- Cadomian long lived (750-540 Ma) Magmatic Arc
Dextral Strike-Slip Faults
ca. >540 Ma
West African Craton
Sahara Meta-Craton
Arabian Nubian Shield
Neoproterozoic Orogenies
Amazonian Craton
Congo Craton
Madagascar
Indian Shield
Kalahari Craton
East Antarctic Shield
Australia Shield
South Pole
C
ca. >540 Ma
1
Mostly 750-540 Ma zircons
Mostly ca. 1.0 Ga zircons
1'
Extinct long lived subduction zone
?
Juvenile Arabian-Nubian rocks with an unknown amount of ca. 1.0Ga igneous rocks
Avalonian- Cadomian long lived (750-550 Ma) Magmatic Arc with an unknown basement
ca. <540 Ma
1
Mostly 750-540 Ma zircons
Mostly ca. 2.0 Ga zircons
1'
Extension and denudation of the Avalonian- CadomianMagmatic Arc with an unknown basement
?
Local exhumation of a ca. 2.0 Ga Basement in the ANS or the Saharan Metacraton

◀**Fig. 9** **a** Plot representing the relative proportion of Tonian–Stenian detrital zircons in different provenance studies performed in different interpreted locations along the northern Gondwana margin. *Letters* indicate the position of the samples studied, in the case they have not been involved in subsequent major orogenic cycles and the interpreted position for those that have been involved in Variscan and/or Alpine cycles. *A*—Anti-Atlas (Morocco), Abati et al. (2010), Avigad et al. (2012); *B*—Ossa-Morena Zone (Iberia), Fernández-Suárez et al. (2002a), Pereira et al. (2012a); *C*—Southern Central Iberian Zone (Iberia), Pereira et al. (2012b); *C*—Southern Central Iberian Zone (Iberia), Pereira et al. (2012b); *D*—Sardinia (Italy), Avigad et al. (2012); *E*—Tassili Ouan Ahaggar (Algeria), Linnemann et al. (2011); *F*—Al Qarqaf Arc (Libya), Altumi et al. (2013); Dor el Gussa (Libya), Meinhold et al. (2011), Ramos et al. (2008); Sicily (Italy), Williams et al. (2012); *H*—Basal Units (NW Iberia), Díez Fernández et al. (2010); *I*—Lower Allochthon (NW Iberia), Díez Fernández et al. (2012), Dias da Silva (2013); *J*—Central Iberian, West Asturian and Cantabrian Zones (NW Iberia). This work and Fernández-Suárez et al. (2000, 2002b), Gutiérrez-Alonso et al. (2003), Martínez Catalán et al. (2004), Shaw et al. (2012a, b), Pastor-Galán et al. (2012a, b), Ábalos et al. (2012); *S*—Sa'al Complex (Sinaí, Egypt), Be'eri-Shlevin et al. (2009); *T*—Southern Israel, Avigad et al. (2003), Kolodner et al. (2006), Eyal et al. (2013); *U*—Jordan, Kolodner et al. (2006); *V*—Egypt, Wilde and Youssef (2002); Bi'ir Umq (Saudi Arabia), Hargrove et al. (2006); *V*—Tigrai (Ethiopia), Avigad et al. (2007); *X*—Ad Dawadimi (Saudi Arabia), Cox et al. (2012); *Z*—Iran, Horton et al. (2008). **b** Tentative paleogeographic reconstruction of Gondwana during the Ediacaran–Cambrian boundary showing the location of the major Neoproterozoic orogenies and the inferred location of terranes for which available detrital zircon U–Pb age data exist for Ediacaran and Paleozoic rocks (references above). *Black stars* indicate locations with documented ca 1.0 Ga igneous rocks in Africa which could be the source rocks for detrital Tonian–Stenian zircons: [Darfur Massif (Tchad–Sudan)—De Wit et al. (2005); Sinaí (Egypt)—Be'eri-Shlevin et al. (2012), Eyal et al. (2013); Eastern Egypt—Loizenbauer et al. (2001); Bayuda desert (Sudan)—Küster et al. (2008); Chewore–Runfusa Terrane (Zambia); Irumide belt—De Waele et al. (2003, 2006); De Waele and Fitzsimons (2007, 2009); Kibaran Belt—Kokonyangi et al. (2004); Namaqua Belt (South Africa)—Eglington (2006); Kalahari (Namibia, South Africa, Botswana)—Singletary et al. (2003); Ribeira Belt (Uruguay)—Basei et al. (2011); Borborema (Brazil)—Van Schmus et al. (2008)]. *White stars* are locations with documented Tonian–Stenian detrital zircons in Neoproterozoic or Lower Paleozoic rocks of Africa [Sabaloka (Sudan)—Kröner et al. (1987); Volta Basin (Ghana)—Kalsbeek et al. (2008); Shakawe (Botswana)—Mapeo et al. (2000); Yaoundé Series (Cameroon)—Ngnotue et al. (2012); South Africa—Fourie et al. (2011); Central Madagascar: Cox et al. (2004)]. **c** Sketch proposing a possible scenario to illustrate the change in tectonic regime from the active margin (back-arc) stage to the onset of the development of a passive margin and the change in local source areas at the Ediacaran–Cambrian boundary. The sketch corresponds to an approximate location close to line 1–1' in Fig. 9b (see text for details)

distributions are not significantly different. KS tests also show that sample OD3 contains a zircon age distribution that is not significantly different from that of samples OD2, OD5 and OD7 in the Narcea Antiform Domain (Fig. 7). However, sample OD3 has a significantly more negative ε_{Nd} and a higher T_{DM} value than sample OD4 (and samples OD2, OD5 and OD7) (Fig. 4c), which indicates a change in the composition of the detrital influx not imaged by the distribution of U–Pb zircon ages.

The data suggest that the Late Ediacaran basin (or basins) in both domains of Iberia were fed from the same source areas and these were essentially unchanged for at least 50 Myr, between ca. 600 and 550 Ma, when the active margin Ediacaran cycle was ending. The data indicate a very abrupt change in the composition of the source area by the Early Cambrian in the Narcea Antiform Domain (OD2 vs. OD1). This change is more subtle in the Central Iberian Zone (OD4 vs. OD3; see also Ábalos et al. 2012), and it is also reflected by the more negative Nd isotopic compositions in OD3. The change may correspond to the documented latest Ediacaran–early Cambrian tectonic activity (unconformity in the Narcea Antiform Domain, olistostromal deposits in the CIZ).

The changes brought about by this tectonic activity may also caused the alongshore changes in the nature of detritus being fed to the early Cambrian basin(s) (OD1 vs. OD3) associated with along-margin transport of different realms or with the local exhumation of basement rocks with different ages.

Possible settings and sources

Samples OD2, OD4, OD5 and OD7 (Ediacaran) have very similar lithogeochemical, Sm–Nd isotopic and U–Pb detrital zircon signatures suggesting derivation from the same source. The geochemical discrimination diagrams (Fig. 4a) suggest that this source was an active island/continental arc, a conclusion consistent with previous geological geochemical and geochronological information (e.g., Fernández-Suárez et al. 2002a, b; Gutiérrez-Alonso et al. 2003; Avigad et al. 2003, 2012; Nance et al. 2008 and references therein; Díez Fernández et al. 2010, 2012; Linnemann et al. 2011; Pereira et al. 2012a, b; Rubio-Ordóñez 2010, in press).

A peri-arc scenario for the deposition of the Ediacaran rocks is also consistent with the limited time gap between the age of the youngest detrital zircon populations and time of deposition. An active margin environment is also consistent with the cumulative distribution of zircon crystallization ages–depositional age (CA–DA) as depicted in Fig. 8 (based on the work by Cawood et al. 2012) where samples OD5 and 7, OD2 and OD4 (Ediacaran) plot in the field of active margin (convergent) settings. Sample OD3 (Lower Cambrian, CIZ) also falls in this field and has a CA–DA cumulative distribution undistinguishable from those of the Ediacaran samples. Sample OD1 has a very different CA–DA cumulative distribution owing to the lack of Tonian–Stenian zircons and the high proportion of Paleoproterozoic zircons. However, based on the criteria of Cawood et al. (2012), this sample still meets the requirements of zircon distributions characteristic of convergent settings (CA–DA < 150 Ma at 5 %

data and CA–DA < 100 Ma at 30 % data). For comparison, we have included a Silurian sample (Formigoso, DA = 435 Ma; Pastor-Galán et al. 2012a, b) and a Devonian sample (Fueyo, DA = 375 Ma), which illustrate the transition from an arc environment in the Ediacaran–Early Cambrian to an extensional (passive margin-stable platform) setting in the Paleozoic in terms of detrital zircon age distribution in relation to depositional age.

The Nd isotopic composition of Ediacaran samples is also compatible with a peri-arc setting where the relatively high $\varepsilon_{Nd(i)}$ (>−3) values (Table 2 in electronic online supplement) are consistent with input of relatively juvenile detrital components. The values of $\varepsilon_{Nd(i)}$ in the Cambrian samples are markedly more negative, with a concomitant increase in the T_{DM} values (see also Gutiérrez-Alonso et al. 2003); this increase is especially pronounced in sample OD1 (which has a very different detrital zircon content) but is also significant in sample OD3 whose detrital zircon content is not significantly different from that of the Ediacaran samples and suggests a more important contribution from older basement rocks, which is not reflected in its zircon content.

Finally, the geochemical and isotopic (Sr, Nd) characteristics of the Ediacaran granitoids intruding the Allande Unit (high Mg, I-type calc-alkaline) are also indicative of an arc setting (see Gutiérrez-Alonso and Fernández-Suárez 1996; Fernández-Suárez et al. 1998; Rubio Ordóñez et al. in press).

Figure 7a shows the results of KS tests between the samples studied herein and the zircon populations of samples from other units in Iberia and other relevant realms in the peri-Gondwanan realm (references in Fig. 7a). The Ediacaran samples (and also the Cambrian sample OD3) have detrital zircon U–Pb age distributions that match those of Lower Cambrian to Lower Ordovician sedimentary rocks from Israel and Jordan in the Arabian Nubian Shield (Kolodner et al. 2006) and are also similar to the zircon populations in the Middle Cambrian strata of Morocco (Avigad et al. 2012). The Ediacaran samples also compare favorably with their correlatives in the southern CIZ (Pereira et al. 2012b) but not with rocks from the Basal Units or the Parautochtonous Units of NW Iberia (Díez Fernández et al. 2010, 2012), which are considered to represent the most outboard sequences in the Ediacaran–Early Paleozoic of Iberia. These differences could be related to their different relative positions along the Gondwana active margin environment and could be explained by the Basal Units and the Parautochtonous sequence (and also the OMZ, see Pereira et al. 2012a) being closer to the Avalonian–Cadomian magmatic arc and further to the west (Fig. 9). In this scenario, the influx of detritus containing Tonian–Stenian zircons would have been smaller and the more westerly location would explain the higher proportion of ca. 2 Ga zircons (Eburnean event) with a northwest Africa Craton provenance.

The presence of abundant zircons in the age range ca. 550–750 Ma, representing the period of Avalonian–Cadomian arc construction along the northern Gondwanan margin (see Nance et al. 2008 and references therein) in all samples, is interpreted to indicate derivation from a local arc source, which is also supported by the ca. 600–750 Ma ^{40}Ar–^{39}Ar ages provided by detrital micas in equivalent rocks (Gutiérrez-Alonso et al. 2005). The ca. 0.85–1.15 Ga population present in all samples except OD1 and also in the samples from Israel and Jordan, and the Middle Cambrian of Morocco and other peri-Gondwanan realms of Iberia and Europe suggests the presence, at the time of deposition, of a volumetrically significant basement source containing ca. 1.0 Ga zircon-bearing rocks. An arc-type terrain is an ideal candidate to have supplied the Tonian–Stenian (0.85–1.15 Ga) zircons to the Ediacaran–Cambrian basins. It should be noted that the proportion of Tonian–Stenian zircons increases significantly in Ordovician to Devonian strata in northern and central Iberia, up to 30–35 % of the total zircon population (Shaw et al. 2012a, b) and in Libya, highlighting the volumetric importance of such a basement arc terrane.

A recent study by Be'eri-Shlevin et al. (2012) proves the existence of such an arc terrane in the Sinai, Egypt (northern Arabian Nubian Shield), whose igneous rocks have ages that match the above detrital zircon age interval (ca. 0.85–1.05 Ga). Terranes like the Sa'al, if proven of wider distribution, would make suitable candidates to constitute the basement source for the Tonian–Stenian zircons found in the Ediacaran and Paleozoic samples of Iberia and other peri-Gondwanan realms.

Rocks of appropriate age also exist in the peri-Rodinian Valhalla orogens (Cawood et al. 2010) but their potential connection to the northern margin of Gondwana in late Ediacaran–Early Cambrian times is not likely in light of currently applied paleogeographic scenarios for this period (Cocks and Torsvik 2006; Meert and Lieberman 2008; Cawood et al. 2010). However, it is not unreasonable to conjecture that both the Valhalla and the Sa'al arc–terranes were generated during the amalgamation or early stages of breakup of Rodinia. One such arc terrane could have been involved in the amalgamation of Gondwana (closure of the Mozambique Ocean? Collins and Pisarevsky 2005; Cox et al. 2012) and later act as a source of detritus to the Ediacaran basins of northern Gondwana.

The absence of ca. 1.2–1.6 Ga Mesoproterozoic zircons in the studied rocks (and also in their peri-Gondwanan correlatives) excludes derivation from Amazonian–Avalonian or Oaxaquian sources as suggested by Fernández-

Suárez et al. (2000) based on the available limited database 10 years ago. The involvement of source rocks from the Kibaran orogens in southern central Africa is also unlikely owing to the absence of zircons in the age range 1.2–1.6 Ga, a feature of the Kibaran rocks (e.g., De Waele et al. 2003 and references therein).

In spite of the above arguments and given the combination of detrital zircon U–Pb ages and detrital mica $^{40}Ar–^{39}Ar$ ages in NW Iberian Ediacaran and Cambrian sedimentary rocks, it is still permissible to conjecture that the source for these rocks is still unmatched by any known basement source terrain.

An additional feature of the data presented herein is the contrast in detrital zircon content and Sm–Nd isotopic signature of sample OD1 with the underlying sample OD2 and with its probable temporal correlative OD3. OD2 and OD3 samples contain Tonian–Stenian zircons similar to the Middle Cambrian clastic rocks from Morocco (where no older rocks contain this age group, cf. Abati et al. 2010; Avigad et al. 2012). Interpretation of the significance of this contrast is further constrained by the presence of Tonian–Stenian (0.95–1.05 Ga) and Statherian (1.6–1.8 Ga) detrital muscovite in sample OD1 (Gutiérrez-Alonso et al. 2005). The detrital zircon content of sample OD1 indicates that the basin in which it was deposited was cut off from the Tonian–Stenian basement rocks and instead was flooded with zircons coming from the arc itself (ca 550–750 Ma zircons) and detritus from Paleoproterozoic and Archean basement rocks such as those present in the West African Craton (ca. 1.9–2.2 and 2.5–2.7 Ga) with a metamorphic or hydrothermal overprint as revealed by the ages provided by the detrital micas.

Unfolding the oroclines that conform the western Iberia orogenic architecture (Martínez Catalán 2011; Shaw et al. 2012a, b), sample OD3 would have been closer to the WAC than OD1 so a change in the drainage system is hard to reconcile with sample OD3 containing Tonian–Stenian zircons and sample OD1 lacking them. More likely, the "OD1 section" of the Cambrian basin was involved in a tectonic event that created a topographic high with rapid denudation of the Tonian–Stenian basement and subsequent exposure of old cratonic areas that flooded the lower Cambrian basin at the time of OD1 deposition, whereas OD3 was deposited in an alongshore section of the basin where this change is hardly perceptible in terms of zircon age distribution (Fig. 9b, c).

Figure 9a shows the relative abundance of Tonian–Stenian zircons in Ediacaran and Paleozoic sedimentary rocks from Iberia and other relevant realms of the northern margin of Gondwana (including northern Africa) for which extensive zircon U–Pb data bases exist. From this figure, it is apparent that relatively abundant (>5 %) Tonian–Stenian zircons occur in the Ediacaran rocks of NW Iberia (northern and central domains of the CIZ, WALZ and CZ) but they are less abundant in the more internal Basal Units and Parautochthonous sequences. In the lower Cambrian, the central Iberian Zone and Israel–Jordan have a significantly higher proportion of Tonian–Stenian zircons than other realms and suggest that the CIZ could be close to those realms which in turn are close to the Sa'al arc terrane but they are apparently absent in parts of central–northern Africa (Libya) and also in sample OD1 (Cantabrian Zone of NW Iberia).

Figure 9b, c is an attempt to summarize the observations arising from this study and to build a platform upon which to add new results and visualize new or refined hypotheses. In these drawings, we suggest that changes in detrital zircon content such as those observed between samples OD2 and OD1 in the Cantabrian Zone could be explained by normal faults on the continent side of the arc, which sank the "Tonian–Stenian" basement and raised older basement sources (i.e., Paleoproterozoic and Archean). Changes in detrital zircon population such as those observed between the Central Iberian–Cantabrian zones (this study) and the Basal Units–Parautochthonous sequences (Díez Fernández et al. 2010, 2012; Pereira et al. 2012a) of Iberia could be explained by their different location with respect to the arc and the continent. And finally, we argue that some kind of strike slip transport (roughly along-margin) must be invoked to allow for the juxtaposition of NW Iberia with the Ossa Morena Zone that may have occurred in latest Ediacaran–earliest Cambrian times (e.g., López-Guijarro et al. 2008) or to explain the presence of Tonian–Stenian zircons in the Middle Cambrian strata of Morocco (Avigad et al. 2012).

Furthermore, there are two rather poorly constrained aspects that need to be addressed in order to understand the linkage of the studied samples with putative provenance areas. First we should understand the nature of the Gondwana amalgamation during the Pan-African orogenic event. One of the big questions regarding this issue is whether the Pan-African orogenic event was caused by the closure of large oceans separating the cratons that shape the geological architecture of central–northern Africa or it represents ensialic deformations that only reworked previous collisional belts. Recent studies favor the former scenario in which the complete amalgamation of Gondwana took place through ocean closure(s) during an extended period of time, Ediacaran in the northern East African orogen (e.g., Stern 1994; Collins and Pisarevsky 2005; Johnson et al. 2011; Cox et al. 2012) to mid-Cambrian in other orogenic tracts located more southerly (e.g., Tohver et al. 2012). The Neoproterozoic closure of large (?) oceans would have involved the generation of magmatic arcs that could be the source of the predominant ca. 540–750 Ma zircons instead of or in addition to the classically assumed northern Gondwana peripheral magmatic arc (note that, as mentioned above, the ca 550–750 Ma age populations of samples OD1 and OD2 are significantly different from one another, see also Pereira et al. 2012b). Furthermore, the peripheral Cadomian Arc could have been developed upon continental rocks involving a ca. 1.0 Ga basement, thus providing a source for the Tonian–Stenian zircons found in the studied rocks.

The second aspect to be taken into account is the paleogeography imposed by the Transgondwanan Supermountain Belt (Squire et al. 2006) and the associated large-scale depositional systems (Meinhold et al. 2013). The topography created by the generation of this large mountain belt could have allowed long distance transport of zircons from rocks located in present-day central Africa to the peri-arc basins through continental-scale drainage systems.

Scenarios involving arc and continent-derived sedimentary influx in a changing tectonic regime may have been further complicated by complex sediment re-distribution patterns akin to those reported from the present-day China sea (Huang and Wang 2006; Kim et al. 2013).

Epilogue

Perhaps a conclusion underlying the results of this study is that detrital zircon U–Pb age data, even in statistically robust data sets, do not provide unique solutions for provenance/paleogeographic riddles. This might be so for a variety of reasons: (1) we do not know enough about the sedimentological control on zircon (heavy mineral) distribution in the sedimentary environment and hence how permissible it is to assume that one or even a few samples from a sedimentary formation are representative of that formation; (2) zircon obviously does not bear information on detrital components derived from non-zircon-bearing rocks, which can be predominant in a source area; (3) rocks bearing very high uranium zircons that will be mostly destroyed during transport, or rocks bearing very small zircons (say <50 μm) that will likely not be analyzed. In addition, because older zircons especially those older than 1.5–1.7 Ga show more pronounced discordance in LA–ICP–MS analyses, the statistical distribution of the "older component" in a population cannot be usually assessed with accuracy (in our current case, it is reasonable to presume that a robust statistics of the Archean zircon content in all considered samples would add valuable information based on what we know of the distribution of Archean terranes in central and northern Africa).

This study strongly suggests that the critical time slice when major changes occurred at different scales on the Gondwanan margin was between ca. 550 and 530 Ma, which includes the Ediacaran–Cambrian boundary, the demise of the long-lived Avalonian–Cadomian arc magmatism, the birth of the Rheic Ocean and the transition to a stable platform on the northern margin of Gondwana. Consequently, further U–Pb (ideally combined with Lu–Hf and oxygen isotopes) on detrital zircons and whole rock Sm–Nd data from the late Ediacaran–early Cambrian formations of the peri-Gondwanan realm are necessary in order to further our understanding of the above-discussed issues. Implicitly, a better stratigraphic correlation of the peri-Gondwanan Ediacaran–Cambrian successions based on tight absolute age constraints would greatly aid these studies.

Acknowledgments J.F.S. wishes to acknowledge the financial support from project CONSOLIDER CGL2007-65338-C02-01/BTE by the Spanish Ministry of Science and Technology. G.G.-A. and D.P.-G. were financially supported by Research Project ODRE II ("Oroclines and Delamination: Relations and Effects") CGL2009-1367 from the Spanish Ministry of Economy and Competitivity. This paper is part of the IGCP Project from UNESCO No. 574: Buckling and Bent Orogens, and Continental Ribbons. Francisco Pereira and Dov Avigad are gratefully acknowledged for constructive and insightful reviews.

References

Abad I, Nieto F, Gutiérrez-Alonso G (2003) Textural and chemical changes in slate-forming phyllosilicates across the external-internal zones transition in the low-grade metamorphic belt of the NW Iberian Variscan Chain. Schweiz Mineral Petrogr Mitt 83:63–80

Ábalos B, Gil Ibarguchi JI, Sánchez-Lorda ME, Paquette J (2012) African/Amazonian Proterozoic correlations of Iberia: A detrital zircon U–Pb study of early Cambrian conglomerates from the Sierra de la Demanda (northern Spain). Tectonics 31. doi: 10.1029/2011TC003041

Abati J, Aghzer A, Gerdes A, Ennih N (2010) Detrital zircon ages of Neoproterozoic sequences of the Moroccan Anti-Atlas belt. Prec Res 181:115–128

Altumi MM, Elicki O, Linnemann U, Hofmann M, Sagawe A, Gärtner A (2013) U-Pb LA-ICP-MS detrital zircon ages from the Cambrian of Al Qarqaf arch, central-western Libya: provenance of the West Gondwanan sand sea at the dawn of the early Palaeozoic. J Afr Earth Sci 79:74–97

Álvaro JJ, Vennin E, Moreno-Eiris E, Perejón A, Bechstädt T (2000) Sedimentary patterns across the Lower-Middle Cambrian transition in the Esla nappe (Cantabrian Mountains, northern Spain). Sediment Geol 137:43–61. doi:10.1016/S0037-0738(00)00134-2

Amidon WH, Burbank DW, Gehrels GE (2005) Construction of detritalmineral populations: insights from mixing of U–Pb zircon ages in Himalayan rivers. Basin Res 17:463–485. doi:10.1111/j.1365-2117.2005.00279.x

Angerer T (2007) Fossil Paleoweathering profiles and their relation to Deformation at Basement-Cover-Interfaces. Case studies from Israel, Sweden and Spain. PhD Thesis, Ruprecht-Karls-Universität Heidelberg, Germany, 273 pp

Aramburu C, Truyols J, Arbizu M, Mendez-Bédia I, Zamarreño I, García-Ramos JC, Suárez de Centi C, Valenzuela M (1992) El Paleozoico Inferior de la Zona Cantábrica. In: Gutiérrez Marco JC, Rábano I, Saavedra J, Rábano I (eds) Paleozoico Inferior de

Iberio-Armérica. University of Extremadura, Extremadura, pp 397–721

Aramburu C, Méndez-Bedia I, Arbizu M (2002) The lower Paleozoic in the Cantabrian zone (Cantabrian Mountains, NW Spain). In: García-López S, Bastida F (eds) Paleozoic conodonts from north Spain, Cuad Mus Geomin 1 35:49

Avigad D, Kolodner K, McWilliams M, Persing H, Weissbrod T (2003) Origin of northern Gondwana Cambrian sandstone revealed by detrital zircon SHRIMP dating. Geology 31:227–230

Avigad D, Stern RJ, Beyth M, Miller N (2007) Detrital zircon U-Pb geochronology of Cryogenian diamictites and Lower Paleozoic sandstone in Ethiopia (Tigrai): age constraints on Neoproterozoic glaciation and crustal evolution of the southern Arabian Nubian Shield. Prec Res 154:88–106

Avigad D, Gerdes A, Morag N, Bechstädt T (2012) Coupled U–Pb–Hf of detrital zircons of Cambrian sandstones from Morocco and Sardinia: implications for provenance and Precambrian crustal evolution of North Africa. Gond Res 21:690–703

Barbeau DL Jr, Davis JT, Murray KE, Valencia V, Gehrels GE, Zahid KM, Gombosi DJ (2009) Detrital-zircon geochronology of the metasedimentary rocks of north-western Graham Land. Antarctic Sci. doi:10.1017/S095410200999054X

Basei MAS, Peel E, Sánchez Bettucci L, Preciozzi F, Nutman AP (2011) The basement of the Punta del Este Terrane (Uruguay): an African Mesoproterozoic fragment at the eastern border of the South American Río de La Plata cratón. Intern J Earth Sci 100:289–304

Bea F, Montero P, Talavera C, Abu Anbar M, Scarrow JH, Molina JF, Moreno JA (2010) The palaeogeographic position of Central Iberia in Gondwana during the Ordovician: evidence from zircon chronology and Nd isotopes. Terra Nova 22:341–346

Be'eri-Shlevin Y, Katzir Y, Whitehouse MJ, Kleinhanns CI (2009) Contribution of pre Pan-African crust to formation of the Arabian Nubian Shield: new secondary ionization mass spectrometry U–Pb and O studies of zircon. Geology 37:899–902

Be'eri-Shlevin Y, Eyal M, Eyal Y, Whitehouse MJ, Litvinovsky B (2012) The Sa'al volcano-sedimentary complex (Sinai, Egypt): a latest Mesoproterozoic volcanic arc in the northern Arabian Nubian Shield. Geology 40:403–406

Ramos E, Fernández-Suárez J, Barsó D, Marzo M, Tawengi KS, Khoja AA, Bolatti, ND (2008) Detrital modes and U–Pb ages of zircons from Middle Ordovician strata of the Murzuq Basin, Libya: Implications for provenance and tectonics of the western Gondwanan margin. 1st MAPG international conference, Marrakech, Morocco, Abstracts, #90074

Carrington da Costa J (1950) Noticia sobre una carta geologica do Buçaco, de Nery Delgado. Com Serv Geol Portugal

Cawood A, Strachan R, Cutts K, Kinny PD, Hand M, Pisarevsky S (2010) Atlantic Neoproterozoic orogeny along the margin of Rodinia: Valhalla orogen, North Atlantic. Geology 38:99–102

Cawood PA, Hawkesworth CJ, Dhuime B (2012) Detrital zircon record and tectonic setting. Geology 40:875–878

Cocks LRM, Torsvik TH (2006) European geography in a global context from the Vendian to the end of the Palaeozoic. In: Gee DG, Stephenson RA (eds) European lithosphere dynamics. Geol Soc Lond Mem 32:83–95

Collins AS, Pisarevsky SA (2005) Amalgamating eastern Gondwana: the evolution of the Circum-Indian Orogens. Earth Sci Rev 71:229–270

Cox R, Coleman DS, Chokel CB, DeOreo SB, Wooden JL, Collins AS, De Waele B, Kröner A (2004) Proterozoic Tectonostratigraphy and paleogeography of Central Madagascar derived from detrital zircon U–Pb age populations. J Geol 112:379–399

Cox GM, Lewis CJ, Collins AS, Halverson GP, Jourdan F, Foden J, Nettle D, Kattan F (2012) Ediacaran terrane accretion within the Arabian–Nubian Shield. Gond Res 21:341–352

de Sitter LU (1961) Le Précambrien dans le Chaîne Cantabrique. C Rend Soc Géol France 9:253

De Waele B, Fitzsimons ICW (2007) The nature and timing of Palaeoproterozoic sedimentation at the southeastern margin of the Congo Craton; zircon U–Pb geochronology of plutonic, volcanic and clastic units in northern Zambia. Prec Res 159: 95–116

De Waele B, Wingate MTD, Mapani B, Fitzsimons ICW (2003) Untying the Kibaran knot: a reassessment of Mesoproterozoic correlations in southern Africa based on SHRIMP U-Pb data from the Irumide belt. Geology 31:509–512

De Waele B, Kampunzu AB, Mapani BSE, Tembo F (2006) The Mesoproterozoic Irumide belt of Zambia. J African Earth Sci 46:36–70

De Waele B, Fitzsimons ICW, Wingate MTD, Tembo F, Mapani B, Belousova EA (2009) The geochronological framework of the Irumide Belt: prolonged crustal history along the margin of the Bangweulu Craton. Am J Sci 309:132–187

de Wit MJ, Bowring S, Dudas F, Kamga G (2005) The great Neoproterozoic CentralSaharan arc and the amalgamation of the North African Shield. GAC-MAC-CSPG-CSSS Joint Meeting, Halifax, Nova Scotia, Abstracts, 30:42–43

DeGraaff-Surpless K, Mahoney JB, Wooden JL, McWilliams MO (2003) Lithofacies control in detrital zircon provenance studies: insights from the Cretaceous Methow basin, southern Canadian Cordillera. Geol Soc Amer Bull 115:899–915

DePaolo DJ (1981) Neodymium isotopes in the Colorado Front Range and crust mantle evolution in the Proterozoic. Nature 291:193–196

DePaolo DJ (1988) Neodymium isotope geochemistry: an introduction. Springer, New York

Dias da Silva I (2013) Geology of the Central Iberian and Galicia-Trás-os-Montes Zones in the Eastern Part of the Morais Complex, Portugal/Spain. PhD thesis, Universidad de Salamanca

Díaz García F (2006) Geometry and regional significance of Neoproterozoic (Cadomian) structures of the Narcea Antiform, NW Spain. J Geol Soc 163:499–508

Dickinson WR, Gehrels GE (2009) U-Pb ages of detrital zircons in Jurassic eolian and associated sandstones of the Colorado Plateau: Evidence for transcontinental dispersal and intraregional recycling of sediment: Geol Soc Amer Bull 121:408–433

Dickinson WR, Lawton TF, Gehrels GE (2009) Recycling detrital zircons: a case study from the Cretaceous Bisbee Group of southern Arizona. Geology 37:503–506

Dickinson WR, Gehrels GE, Stern RJ (2010) Late Triassic Texas uplift preceding Jurassic opening of the Gulf of Mexico: evidence from U–Pb ages of detrital zircons. Geosphere 6: 641–662

Díez Balda MA (1986) El complejo esquisto-grauváquico, las series paleozoicas y la estructura hercínica al Sur de Salamanca. Ediciones Universidad de Salamanca, 162 pp

Díez Fernández R, Martínez Catalán JR, Gerdes A, Abati J, Arenas R, Fernández-Suárez J (2010) U-Pb ages of detrital zircons from the Basal allochthonous units of NW Iberia: provenance and paleoposition on the northern margin of Gondwana during the Neoproterozoic and Paleozoic. Gondwana Res 18:385–399

Díez Fernández R, Martínez Catalán JR, Arenas R, Abati J, Gerdes A, Fernández-Suárez J (2012) U–Pb detrital zircon analysis of the lower allochthon of NW Iberia: age constraints, provenance and links with the Variscan mobile belt and Gondwanan cratons. J Geol Soc 169:655–665

Dostal J, Dupuy C, Caby R (1994) Geochemistry of the Neoproterozoic Tilemsi belt of Iforas (Mali, Sahara): a crustal section of an oceanic island arc. Prec Res 65:55–69

Eglington BM (2006) Evolution of the Namaqua-Natal Belt, southern Africa—a geochronological and isotope geochemical review. J Afr Earth Sci 46:93–111

Eyal M, Be'eri-Slevin Y, Eyal Y, Whitehouse MJ, Litvinovsky B (2013) Three successive Proterozoic island arcs in the Northern Arabian-Nubian Shield: Evidence from SIMS U-Pb dating of zircon. Gondwana Res. doi:10.1016/j.gr.2013.03.016

Fernández-Suárez J, Gutiérrez-Alonso G, Jenner GA, Jackson SE (1998) Geochronology and geochemistry of the Pola de Allande granitoids (northern Spain). Their bearing on the Cadomian/Avalonian evolution of NW Iberia. Can J Earth Sci 35: 1439–1453

Fernández-Suárez J, Gutiérrez-Alonso G, Jenner GA, Tubrett MN (1999) Crustal sources in Lower Palaeozoic rocks from NW Iberia: insights from laser ablation U–Pb ages of detrital zircons. J Geol Soc 156:1065–1068

Fernández-Suárez J, Gutiérrez-Alonso G, Jenner GA, Tubrett MN (2000) New ideas on the Proterozoic–Early Palaeozoic evolution of NW Iberia: insights from U–Pb detrital zircon ages. Prec Res 102:185–206

Fernández-Suárez J, Gutiérrez-Alonso G, Jeffries TE (2002a) The importance of along-margin terrane transport in northern Gondwana: insights from detrital zircon parentage in Neoproterozoic rocks from Iberia and Brittany. Earth Planet Sci Lett 204:75–88

Fernández-Suárez J, Gutiérrez-Alonso G, Cox R, Jenner GA (2002b) Assembly of the Armorica microplate: a strike-slip terrane delivery? Evidence from U–Pb ages of detrital zircons. J Geol 110:619–626

Fourie PH, Zimmermann U, Beukes NJ, Naidoo T, Kobayashi K, Kosler J, Nakamura E, Tait J, Theron JN (2011) Provenance and reconnaissance study of detrital zircons of the Palaeozoic Cape Supergroup in South Africa: revealing the interaction of the Kalahari and Río de la Plata cratons. Intern J Earth Sci 100(527):541

Frei D, Gerdes A (2009) Accurate and precise in situ zircon U-Pb age dating with high spatial resolution and high sample throughput by automated LA-SF-ICP-MS. Chem Geol 261:261–270

Gómez Barreiro J, Martínez Catalán JR, Arenas R, Castiñeiras P, Abati J, Díaz García F, Wijbrans J (2007) Tectonic evolution of the upper allochthon of the Órdenes complex (northwestern Iberian Massif): structural constraints to a polyorogenic peri-Gondwanan terrane. In: Linnemann U, Nance RD, Kraft P, Zulauf G (eds) The evolution of the Rheic Ocean: from Avalonian-Cadomian active margin to Alleghenian-Variscan collision. Geol Soc Am Spec Paper 423:315–332

Gozalo R, Liñán E, Palacios T, Gámez Vintaned JA, Mayoral E (2003) The Cambrian of the Iberian Peninsula: an overview. Geol Acta 1:103–112

Gutiérrez-Alonso G (1996) Strain partitioning in the footwall of the Somiedo Nappe: structural evolution of the Narcea Tectonic window, NW Spain. J Struct Geol 18:1217–1229

Gutiérrez-Alonso G, Fernández-Suárez J (1996) Geología y geoquímica del granitoide pre-varisco de Puente de Selce (Antiforme del Narcea, Asturias). Rev Soc Geol España 9:228–239

Gutiérrez-Alonso G, Nieto F (1996) White-mica "crystallinity", finite strain and cleavage development across a large Variscan structure, NW Spain. J Geol Soc 153:287–299

Gutiérrez-Alonso G, Fernández-Suárez J, Jeffries TE, Jenner GA, Tubrett MN, Cox R, Jackson SE (2003) Terrane accretion and dispersal in the northern Gondwana margin. An early Paleozoic analogue of a long-lived active margin. Tectonophysics 365:221–232

Gutiérrez-Alonso G, Fernández-Suárez J, Jeffries TE (2004) Age and setting of the Upper Neoproterozoic Narcea Antiform volcanic rocks (NW Iberia). Geogaceta 35:79–83

Gutiérrez-Alonso G, Fernández-Suárez J, Collins AS, Abad I, Nieto F (2005) Amazonian Mesoproterozoic basement in the core of the ibero-Armorican Arc: Ar-40/Ar-39 detrital mica ages complement the zircon's tale. Geology 33:637–640

Gutiérrez-Marco JC, Aramburu C, Arbizu M, Bernardez E, Hacar Rodríguez MP, Méndez-Bedia I, Montesinos Lopez R, Rabano I, Truyols J, Villas E (1999) Revisión bioestratigráfica de las pizarras del Ordovícico Medio en el noroeste de España (zonas Cantábrica, Asturoccidental-Leonesa y Centroibérica septentrional). Acta Geol Hisp 34:3–87

Hargrove US, Stern RJ, Kimura JI, Manton WI, Johnson PR (2006) How juvenile is the Arabian–Nubian Shield? Evidence from Nd isotopes and pre-Neoproterozoic inherited zircon in the Bi'r Umq suture zone, Saudi Arabia. Earth Planet Sci Lett 252: 308–326

Horton BK, Hassanzadeh J, Stockli DF, Axen GJ, Gillis RJ, Guest B, Amini A, Fakhari MD, Zamanzadeh SM, Grove M (2008) Detrital zircon provenance of Neoproterozoic to Cenozoic deposits in Iran: implications for chronostratigraphy and collisional tectonics. Tectonophysics 451:97–122

Huang W, Wang P (2006) Sediment mass distribution in the South China Sea since the Oligocene. Sci China, Ser D Earth Sci 49:1147–1155

Jensen S, Palacios T, Martí Mus M (2010) Revised biochronology of the Lower Cambrian of the Central Iberian zone, Southern Iberian massif, Spain. Geol Mag 147:690–703

Johnson PR, Andresen A, Collins AS, Fowler AR, Fritz H, Ghebreab W, Kusky T, Stern RJ (2011) Late Cryogenian-Ediacaran history of the Arabian-Nubian Shield: a review of depositional, plutonic, structural, and tectonic events in the closing stages of the northern East African Orogen. J African Earth Sci 61:167–232

Julivert M, Martínez García E (1967) Sobre el contacto entre el Cámbrico y el Precámbrico en la parte meridional de la Cordillera Cantábrica y el papel del Precámbrico en la orogénesis herciniana. Acta Geol Hisp 2:107–110

Julivert M, Fontboté JM, Ribeiro A, Nabais-Conce LE (1972) Mapa tectónico de la Península Ibérica y Baleares 1:1.000.000. IGME Mem 113

Kalsbeek F, Frei D, Affaton P (2008) Constraints on provenance, stratigraphic correlation and structural context of the Volta basin, Ghana, from detrital zircon geochronology: an Amazonian connection? Sediment Geol 212:86–95

Kerr A, Jenner GA, Fryer BJ (1995) Sm–Nd isotopic geochemistry of Precambrian to Paleozoic granitoid suites and the deep-crustal structure of the southeast margin of the Newfoundland Appalachians. Can J Earth Sci 32:224–245

Kim W, Doh SJ, Yu Y, Lee YI (2013) Magnetic evaluation of sediment provenance in the northern East China Sea using fuzzy c-means cluster analysis. Marine Geol. doi:10.1016/j.margeo.2013.01.001

Kokonyangi J, Armstrong R, Kampunzu AB, Yoshida M, Okudaira T (2004) U-Pb zircon geochronology and petrology of granitoids from Mitwaba (Katanga, Congo): implications for the evolution of the Mesoproterozoic Kibaran belt. Prec Res 132:79–106

Kolodner K, Avigad D, McWilliams M, Wooden JL, Weissbrod T, Feinstein S (2006) Provenance of north Gondwana Cambrian–Ordovician sandstone: U-Pb SHRIMP dating of detrital zircons from Israel and Jordan. Geol Mag 143:367–391

Kröner A, Stern RJ, Dawoud AS, Compston W, Reichmann T (1987) The Pan-African continental margin in northeastern Africa: evidence from a geochronological study of granulites at Sabaloka, Sudan. Earth Planet Sci Lett 85:91–104

Küster D, Liégeois JP, Matukov D, Sergeev S, Lucassen F (2008) Zircon geochronology and Sr, Nd, Pb isotope geochemistry of granitoids from Bayuda Desert and Sabaloka (Sudan): evidence for a Bayudian event (920–900 Ma) preceding the Pan-African orogenic cycle (860–590 Ma) at the eastern boundary of the Saharan Metacraton. Prec Res 164:16–39

Linnemann U, Ouzegane K, Drareni A, Hofmann M, Becker S, Gärtner A, Sagawe A (2011) Sands of West Gondwana: an archive of secular magmatism and plate interactions—a case study from the Cambro-Ordovician section of the Tassili Ouan Ahaggar (Algerian Sahara) using U–Pb–LA-ICP-MS detrital zircon ages. Lithos 123:188–203

Loizenbauer J, Wallbrecher E, Fritz H, Meumayr P, Khudeir AA, Kloetzli U (2001) Structural geology, single zircon ages and fluid inclusion studies of the Meatiq metamorphic core complex: implications for Neoproterozoic tectonics in the Eastern Desert of Egypt. Prec Res 110:357–383

Longerich HP, Jenner GA, Fryer BJ, Jackson SE (1990) Inductively coupled plasma-mass spectrometric analysis of geological samples: a critical evaluation based on case studies. Chem Geol 83:105–118

López-Guijarro R, Armendáriz M, Quesada C, Fernández-Suárez J, Murphy JB, Pin C, Bellido F (2008) Ediacaran-Palaeozoic tectonic evolution of the Ossa Morena and Central Iberian zones (SW Iberia) as revealed by Sm-Nd isotope systematics. Tectonophys 461:202–214

Ludwig KR (1998) On the treatment of concordant Uranium-Lead ages. Geochim Cosmochim Acta 62:665–676

Ludwig KR (2009) Isoplot v. 3.71: a geochronological toolkit for Microsoft Excel: Berkeley, California, Berkeley Geochronology Center Special Publication 4

Mapeo RBM, Kampunzu AB, Armstrong RA (2000) Ages of detrital zircon grains from Neoproterozoic siliciclastic rocks in the Shakawe area: implications for the evolution of Proterozoic crust in northern Botswana. South Afr J of Geol 103:156–161

Marcos A, Farias P (1999) La estructura de las láminas inferiores del Complejo de Cabo Ortegal y su autóctono en el área de Chantada (Galicia, NO de España). Trab Geol 21:201–218

Martínez Catalán JR (1985) Estratigrafía y estructura del Domo de Lugo (Sector Oeste de la Zona Asturoccidental-leonesa). Corpus Geologicum Gallecieae 2:1–291

Martínez Catalán JR (2011) Are the oroclines of the Variscan belt related to late Variscan strike-slip tectonics? Terra Nova 23:241–247

Martínez Catalán JR (2012) The Central Iberian arc, an orocline centered in the Iberian Massif and some implications for the Variscan belt. Intern J Earth Sci 101:1299–1314

Martínez Catalán JR, Arenas R, Díaz García F, Abati J (1999) Allochthonous units in the Variscan belt of NW Iberia. Terranes and accretionary history. In: Sinha AK (ed) Basement Tectonics 13:65–84

Martínez Catalán JR, Arenas R, Díaz-Balda MA (2003) Large extensional structures developed during emplacement of a crystalline thrust sheet: the Mondoñedo nappe (NW Spain). J Struct Geol 25:1815–1839

Martínez Catalán JR, Fernández-Suárez J, Jenner GA, Belousova E, Díez Montes A (2004) Provenance constraints from detrital zircon U–Pb ages in the NW Iberian Massif: implication for Palaeozoic plate configuration and Variscan evolution. J Geol Soc 161:463–476

Martínez Catalán JR et al (2007) Space and time in the tectonic evolution of the northwestern Iberian Massif. Implications for the comprehension of the Variscan belt. In: Hatcher RD Jr, Carlson MP, McBride JH, Martínez Catalán JR (eds) 4-D framework of continental crust. Geol Soc Am Mem 200: 403–423

Martínez-Catalán JR, Arenas R, Díaz-García F, Abati J (1997) Variscan accretionary complex of NW Iberia: terrane correlation and succession of tectonothermal events. Geology 25:1103–1106

Meert JG, Lieberman BS (2008) The Neoproterozoic assembly of Gondwana and its relationship to the Ediacaran–Cambrian radiation. Gond Res 14:5–21

Meinhold G, Morton AC, Fanning CM, Frei D, Howard JP, Phillips RJ, Strogen D, Whitham AG (2011) Evidence from detrital zircons for recycling of Mesoproterozoic and Neoproterozoic crust recorded in Paleozoic and Mesozoic sandstones of southern Libya. Earth Planet Sci Lett 312:164–175

Meinhold G, Morton AC, Avigad D (2013) New insights into peri-Gondwana paleogeography and the Gondwana super-fan system from detrital zircon U–Pb ages. Gond Res 23:661–665

Murphy JB, Nance RD (2002) Nd–Sm isotopic systematics as tectonic tracers: an example from West Avalonia, Canadian Appalachians. Earth Sci Rev 59:77–100

Nance RD, Murphy JB, Strachan RA, Keppie JD, Gutiérrez-Alonso G, Fernández-Suárez J, Quesada C, Linnemann U, D'Lemos R, Pisarevsky SA (2008) Neoproterozoic-early Paleozoic tectonostratigraphy and palaeogeography of the peri-Gondwanan terranes: Amazonian v. West African connections. In: Ennih N, Liégeois JP (eds) The boundaries of the West African Craton. Geol Soc Lond Spec Pub 297:345–383

Nance RD, Gutiérrez-Alonso G, Keppie JD, Linnemann U, Murphy JB, Quesada C, Strachan RA, Woodcock NH (2010) Evolution of the Rheic Ocean. Gond Res 17:194–222

Ngnotue T, Ganno S, Nzenti JP, Schulz B, Tchaptchet TD, Shu CE (2012) Geochemistry and Geochronology of Peraluminous High-K Granitic Leucosomes of Yaoundé Series (Cameroon): evidence for a Unique Pan-African Magmatism and Melting Event in North Equatorial Fold Belt. Intern J Geosci 3:525–548

Palacios T, Vidal G (1992) Lower Cambrian acritarchs from northern Spain: the Precambrian-Cambrian Boundary and biostratigraphic implications. Geol Mag 129:421–436

Pastor-Galán D, Gutiérrez-Alonso G, Meere P, Mulchrone K (2009) Factors affecting finite strain estimation in low-grade, low-strain clastic rocks. J Struct Geol 31:1586–1596

Pastor-Galán D, Gutiérrez-Alonso G, Mulchrone KF, Huerta P (2012a) Conical folding in the core of an orocline. A geometric analysis from the Cantabrian Arc (Variscan Belt of NW Iberia). J Struct Geol 39:210–223

Pastor-Galán D, Gutiérrez-Alonso G, Murphy JB, Fernández-Suárez J, Hofmann M, Linnemann U (2012b) Provenance analysis of the Paleozoic sequences of the northern Gondwana margin in NW Iberia: passive margin to Variscan collision and orocline development. Gond Res 23:1089–1103

Pereira MF, Solá AR, Chichorro M, Lopes L, Gerdes A, Silva JB (2012a) North-Gondwana assembly, break-up and paleogeography: U-Pb isotope evidence from detrital and igneous zircons of Ediacaran and Cambrian rocks of SW Iberia. Gond Res 22:866–881

Pereira MF, Linnemann U, Hofmann M, Chichorro M, Solá AR, Medina J, Silva JB (2012b) The provenance of Late Ediacaran and Early Ordovician siliciclastic rocks in the Southwest Central Iberian Zone: constraints from detrital zircon data on northern Gondwana margin evolution during the late Neoproterozoic. Prec Res 192–195:166–189

Pérez-Estaún A, Martínez-Catalán JR, Bastida F (1991) Crustal thickening and deformation sequence in the footwall to the suture of the Variscan Belt of northwest Spain. Tectonophysics 191:243–253

Quesada C (1990) Precambrian terranes in the Iberian Variscan foldbelt. In: Strachan RA, Taylor GK (eds) Avalonian and Cadomian geology of the North Atlantic. Blackie and Son, Glasgow, pp 109–133

Quesada C, Bellido F, Dallmeyer RD, Gil Ibarguchi JI, Oliveira JT, Pérez Estaún A, Ribeiro A, Robardet M, Silva JB (1991) Terranes within the Iberian Massif: correlations with West African sequences. In: Dallmeyer RD, Lecorché JP (eds) The West African Orogens and Circum—Atlantic Correlations. Springer, Berlin, pp 267–294

Ribeiro A, Pereira E, Dias R (1990) Structure in the NW of the Iberian Peninsula. In: Dallmeyer RD, Martínez-García E (eds) Pre-Mesozoic geology of Iberia. Springer, Berlin, pp 221–236

Robardet M (2002) Alternative approach to the Variscan Belt in Southwestern Europe: preorogenic paleobiogeographical constraints. In: Martínez-Catalán JR, Hatcher Jr. RD, Arenas R, Díaz García F (eds) Variscan–Appalachian Dynamics: The Building of the Late Paleozoic Basement. Geol Soc Am Spec Papers 364:1–15

Robardet M (2003) The Armorica "microplate": fact or fiction? Critical review of the concept and contradictory paleobiogeographical data. Palaeogeogr Palaeoclimatol Palaeoecol 195:125–148

Robardet M, Gutiérrez-Marco JC (1990) Sedimentary and faunal domains in the Iberian Peninsula during lower Paleozoic times. In: Dallmeyer RD, Martínez García E (eds) Pre-mesozoic geology of Iberia. Springer, Berlin, pp 383–395

Rodríguez Alonso MD (1985) El complejo esquistoso-grauwáckico y el Paleozoico en el centro-oeste español. Acta Salmanticensia Ciencias 51:1–174

Rodríguez Alonso MD, Alonso Gavilán G (eds) (1995) Neoproterozoic–Lower Cambrian in the central-western part of the Iberian Peninsula. In: Post-conference field guide, XIII geological meeting on the West of the Iberian Peninsula

Rodríguez-Alonso MD, Peinado M, López-Plaza M, Franco P, Carnicero A, Gonzalo JC (2004) Neoproterozoic–Cambrian synsedimentary magmatism in the Central Iberian Zone (Spain): geology, petrology and geodynamic significance. Intern J Earth Sci 93:897–920

Rubio-Ordóñez A (2010) Magmatismo Neoproterozoico Calcoalcalino en el Antiforme del Narcea, PhD Thesis. Departamento de Geología. Universidad de Oviedo

Rubio-Ordóñez A, Barba P, Cuesta A, Gallastegui G, Suárez O, Ugidos JM, Valladares MI (2004) Los cantos volcánicos del conglomerado basal de la Fm. Herrería: evidencias de un Volcanismo Neoproterozoico en la base del Cámbrico. Geogaceta 35:11–14

Rubio-Ordóñez A, Valverde-Vaquero P, González-Menéndez L, Gallastegui G, Cuesta A (in press) Neoproterozoic plutono-volcanic complex in NW Iberia; petrology and geochemical characterization of an arc-related magmatism. Prec Res

Samson SD, D'Lemos RS, Miller BV, Hamilton MA (2005) Neoproterozoic palaeogeography of the Cadomia and Avalon terranes: constraints from detrital zircon U–Pb ages. J Geol Soc 162:65–71

Sánchez Martínez S, Arenas R, Fernández-Suárez J, Jeffries TE (2009) From Rodinia to Pangaea: ophiolites from NW Iberia as witness for a long-lived continental margin. In: Murphy JB, Keppie JD Hynes AJ (eds) Ancient orogens and modern analogues. Geol Soc Spec Pub 327:317–341

Shaw J, Johnston ST, Gutiérrez-Alonso G, Weil AB (2012a) Oroclines of the Iberian Variscan belt: Paleocurrent analysis, U-Pb detrital zircon age dating, and paleogeographic implications. Geotemas 13

Shaw J, Johnston ST, Gutiérrez-Alonso G, Weil AB (2012b) Oroclines of the Variscan orogen of Iberia: paleocurrent analysis and paleogeographic implications. Earth Planet Sci Lett 329–330:60–70

Singletary SJ, Hanson RE, Martin MW, Crowley JL, Bowring SA, Key RM, Ramokate LV, Direng BB, Krol MA (2003) Geochronology of basement rocks in the Kalahari Desert, Botswana, and implications for regional Proterozoic tectonics. Prec Res 121:47–71

Sircombe KN (2004) Age display: an excel workbook to evaluate and display univariate geochronological data using binned frequency histograms and probability density distributions. Comput Geosci 30:21–31

Squire RJ, Campbell IH, Allen CM, Wilson CJL (2006) Did the Transgondwanan Supermountain trigger the explosive radiation of animals on Earth? Earth Planet Sci Lett 250:116–133

Steiger RH, Jäger E (1977) Subcommission on geochronology: convention on the use of decay constants in geo- and cosmochronology. Earth Planet Sci Lett 36:359–362

Stern RJ (1994) Arc assembly and continental collision in the Neoproterozoic East African Orogen: implications for the assembly of Gondwanaland. Ann Rev Earth Planet Sci 22:319–351

Tohver E, Cawood PA, Rossello EA, Jourdan F (2012) Closure of the Clymene Ocean and formation of West Gondwana in the Cambrian: evidence from the Sierras Australes of the southernmost Río de la Plata craton, Argentina. Gond Res. doi:10.1016/j.gr.2011.04.001

Ugidos JM, Armenteros I, Barba P, Valladares MI, Colmenero JR (1997a) Geochemistry and petrology of recycled orogen-derived sediments: a case study from Upper Precambrian siliciclastic rocks of the Central Iberian Zone, Iberian Massif, Spain. Prec Res 84:163–180

Ugidos JM, Valladares MI, Recio C, Rogers G, Fallick AE, Stephens WE (1997b) Provenance of Upper Precambrian–Lower Cambrian shales in the Central Iberian Zone, Spain: evidence from a chemical and isotopic study. Chem Geol 136:55–70

Ugidos JM, Bilstrom K, Valladares MI, Barba P (2003a) Geochemistry of the Upper Neoproterozoic and Lower Cambrian siliciclastic rocks and U-Pb dating on detrital zircons in the Central Iberian Zone, Spain. Intern J Earth Sci 92:661–676

Ugidos JM, Valladares MI, Barba P, Ellam RM (2003b) The Upper Neoproterozoic-Lower Cambrian of the Central Iberian Zone, Spain: chemical and isotopic (Sm–Nd) evidence that the sedimentary succession records an inverted stratigraphy of its source. Geochim Cosmochim Acta 67:2615–2629

Ugidos JM, Sánchez-Santos JM, Barba P, Valladares MI (2010) Upper Neoproterozoic series in the Central Iberian, Cantabrian and West Asturian Leonese Zones (Spain): geochemical data and statistical results as evidence for a shared homogenised source area. Prec Res 178:51–58

Valladares MI (1995) Siliciclastic-carbonate slope apron in an immature tensional margin (Upper Precambrian–Lower Cambrian), Central Iberian Zone, Salamanca, Spain. Sedimentary Geol 94:165–186

Valladares MI, Barba P, Colmenero JR, Armenteros I, Ugidos JM (1998) La sucesión sedimentaria del Precámbrico Superior-Cámbrico Inferior en el sector central de la Zona Centroibérica: litoestratigrafía, geoquímica y facies sedimentarias. Rev Soc Geol España 11:271–283

Valladares MI, Barba P, Ugidos JM, Colmenero JR, Armenteros I (2000) Upper Neoproterozoic–Lower Cambrian sedimentary successions in the Central Iberian Zone (Spain): sequence stratigraphy, petrology and chemostratigraphy. Implications for other European zones. Intern J Earth Sci 89:2–20

Valladares MI, Barba P, Ugidos JM, Colmenero JR (2002) Contrasting geochemical features of the central Iberia shales (Iberian massif, Spain): implications for the evolution of Neoproterozoic-Lower Cambrian sediments and their sources in other peri-Gondwanan areas. Tectonophysics 352:121–132

Valladares MI, Ugidos JM, Barba P, Fallick AE, Ellam RM (2006) Oxygen, carbon and strontium isotope records of Ediacaran carbonates in Central Iberia (Spain). Prec Res 147:354–365

Van Schmus WR, Oliveira EP, da Silva Filho AF, Toteu SF, Penaye J, Guimaraes IP (2008) Proterozoic links between the Borborema Province, NE Brazil, and the Central African Fold Belt. In: Pankhurst RJ, Trouw RAJ, Brito Neves BB, De Wit MJ (eds) West Gondwana: Pre-Cenozoic correlations across the South Atlantic Region. Geol Soc Spec Pub 294: 69–99

Vermeesch P (2004) How many grains are needed for a provenance study? Earth Planet Sci Lett 224:441–451

Vermeesch P (2012) On the visualisation of detrital age distributions. Chem Geol 312–313:190–194
Vidal G, Palacios T, Gámez-Vintaned JA, Díez Balda MA, Grants SWF (1994) Neoproterozoic-early Cambrian geology and paleontology of Iberia. Geol Mag 131:729–756
Vidal G, Palacios T, Moczydlowska M, Gubanov A (1999) Age constraints from small shelly fossils on the early Cambrian terminal Cadomian phase in Iberia. GGF 121:137–143
Weil AB, Van der Voo R, van der Pluijm BA (2001) Oroclinal bending and evidence against the Pangea megashear: the Cantabria–Asturias arc (northern Spain. Geology 29:991–994
Weil AB, Gutiérrez-Alonso G, Conan J (2010) New time constraints on lithospheric scale oroclinal buckling of the Ibero-Armorican arc: a palaeomagnetic study of earliest Permian rocks from Iberia. J Geol Soc 167:127–143
Weil AB, Gutiérrez-Alonso G, Wicks D (2013a) Investigating the kinematics of local thrust sheet rotation in the limb of an orocline: a paleomagnetic and structural analysis of the Esla tectonic unit, Cantabrian–Asturian Arc, NW Iberia. Intern J Earth Sci 102:43–60
Weil AB, Gutiérrez-Alonso G, Johnston ST, Pastor-Galán D (2013b) Kinematic constraints on buckling a lithospheric-scale orocline along the northern margin of Gondwana: a geologic synthesis. Tectonophys 582:25–49
Wilde SA, Youssef K (2002) A re-evaluation of the origin and setting of the late Precambrian Hammamat Group based on SHRIMP U–Pb dating of detrital zircons from Gebel Umm Tawat, North Eastern Desert, Egypt. J Geol Soc 159:595–604
Williams IS, Fiannacca P, Cirrincione R, Pezzino A (2012) Peri-Gondwanan origin and early geodynamic history of NE Sicily: a zircon tale from the basement of the Peloritani Mountains. Gond Res 22:855–865
Wotte T (2009) Re-interpretation of a Lower–Middle Cambrian West Gondwanan ramp depositional system: a case study from the Cantabrian Zone (NW Spain). Facies 55:473–487
Zamarreño I (1972) Las litofacies carbonatadas del Cámbrico de la Zona Cantábrica (NW de España) y su distribución paleogeográfica. Trab Geol Univ Oviedo 5:1–118